



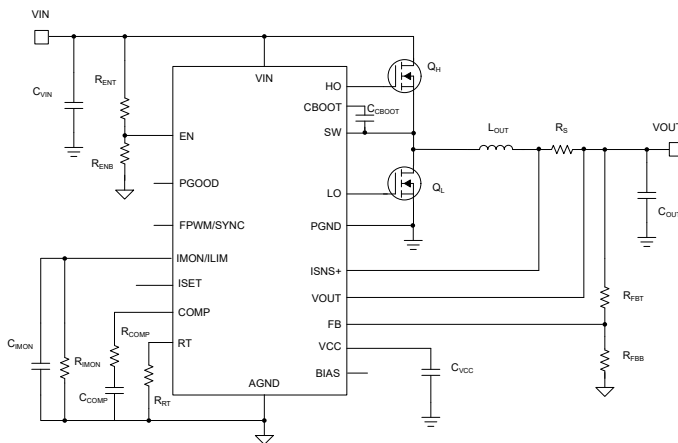
**THE DATASHEET OF  
MT9101A**



# LM25190 42V, Synchronous, Buck Controller With Constant-Current and Constant-Voltage Regulation

## 1 Features

- **Functional Safety-Capable**
  - Documentation available to aid functional safety system design
- Wide input voltage operating range: 5V to 42V
- Adjustable output voltage from 0.8V to 41V, or fixed output of 5V or 12V
- Constant-Current Constant-Voltage (CC-CV) operation
  - Current regulation accuracy:  $\pm 3\%$
  - Voltage regulation accuracy:  $\pm 1\%$
- Current monitoring and constant current features
  - Analog voltage proportional to output current (IMON)
  - Programmable average output current limit (ILIM)
  - Dynamic average output current limit (ISET)
- 2.3 $\mu$ A typical shutdown mode  $I_Q$  and 15 $\mu$ A typical sleep mode  $I_Q$
- Standard level MOSFET gate drivers
- Power-good status indicator (PGOOD)
- Programmable switching frequency from 100kHz to 2.2MHz
- Optional external clock synchronization
- Selectable Dual Random Spread Spectrum (DRSS) feature for enhanced EMI performance across low and high-frequency bands
- Internal slope compensation and bootstrap diode
- Dual-input VCC regulator to reduce power dissipation (BIAS)



Typical Application Schematic

## 2 Applications

- Super capacitor energy backup
- USB power delivery
- Portable power station
- Power tools
- Energy storage system
- Solar energy

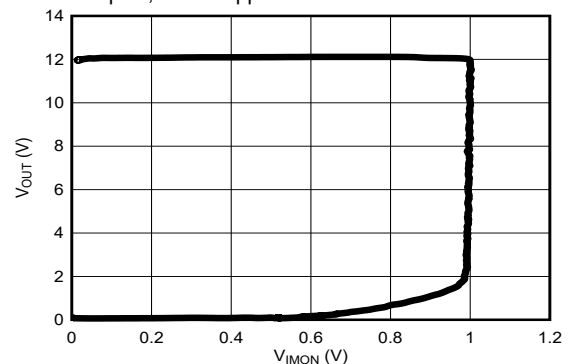
## 3 Description

The LM25190 is an 42V, ultra-low  $I_Q$ , synchronous buck DC/DC controller with Constant-Current Constant-Voltage (CC-CV) regulation. The controller uses a peak current-mode control architecture for easy loop compensation, fast transient response, and excellent load and line regulation. The integrated CC-CV operation features a high accuracy for the regulation of both voltage ( $\pm 1\%$ ) and current ( $\pm 3\%$ ). The CC-CV operation also provides seamless transition between constant-current and constant-voltage mode. The CC-CV operation effectively reduces the Bill Of Materials (BOM) count and cost for applications that require average output current control. The output current limit is programmable and can be dynamically changed. The LM25190 has an output current monitor.

### Package Information

PART NUMBER	PACKAGE <sup>(1)</sup>	PACKAGE SIZE <sup>(2)</sup>
LM25190	RGY (VQFN, 19)	3.5mm × 4.5mm

- (1) For more information, see [Section 10](#).
- (2) The package size (length × width) is a nominal value and includes pins, where applicable.



Constant-Current Constant-Voltage Operation During a Charging Transient



The LM25190 has a unique EMI (Electromagnetic Interference) reduction feature known as [Dual Random Spread Spectrum \(DRSS\)](#). Combining low-frequency triangular and high-frequency random modulations mitigates EMI disturbances across lower and higher frequency bands, respectively. This hybrid technique aligns with the multiple resolution bandwidth (RBW) settings specified in industry-standard EMC tests.

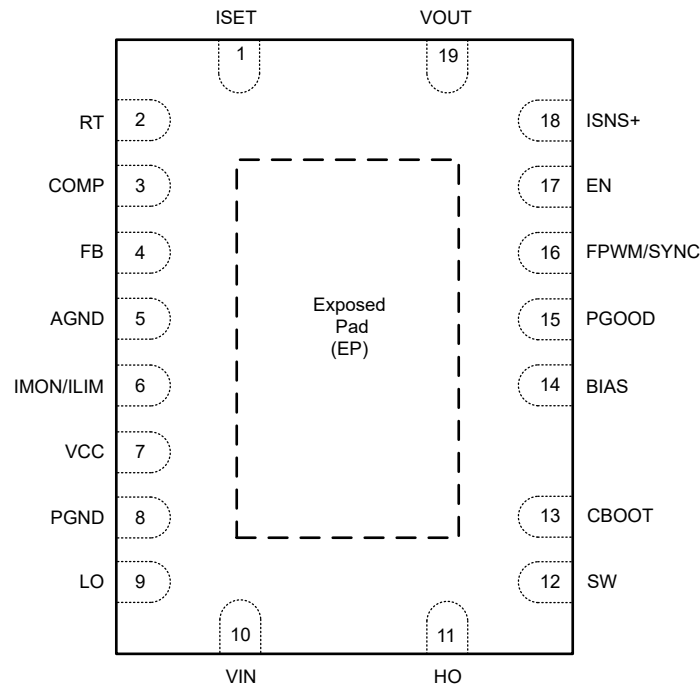
Additional features of the LM25190 include 150°C maximum junction temperature operation, user-selectable diode emulation for lower current consumption at light-load conditions, open-drain power-good flag for fault reporting and output monitoring, precision enable input, monotonic start-up into prebiased load, integrated dual-input VCC bias supply regulator, internal 2.75ms soft-start time, and thermal shutdown protection with automatic recovery.

The LM25190 controller comes in a 3.5mm × 4.5mm, thermally enhanced, 19-pin VQFN package.

## Table of Contents

<b>1 Features</b> .....	<b>1</b>	<b>7 Application and Implementation</b> .....	<b>24</b>
<b>2 Applications</b> .....	<b>1</b>	7.1 Application Information.....	24
<b>3 Description</b> .....	<b>1</b>	7.2 Typical Applications.....	31
<b>4 Pin Configuration and Functions</b> .....	<b>4</b>	7.3 Power Supply Recommendations.....	37
<b>5 Specifications</b> .....	<b>6</b>	7.4 Layout.....	37
5.1 Absolute Maximum Ratings.....	6	<b>8 Device and Documentation Support</b> .....	<b>42</b>
5.2 ESD Ratings.....	6	8.1 Device Support.....	42
5.3 Recommended Operating Conditions.....	6	8.2 Documentation Support.....	42
5.4 Thermal Information.....	7	8.3 Receiving Notification of Documentation Updates....	43
5.5 Electrical Characteristics.....	7	8.4 Support Resources.....	43
5.6 Typical Characteristics.....	9	8.5 Trademarks.....	43
<b>6 Detailed Description</b> .....	<b>12</b>	8.6 Electrostatic Discharge Caution.....	43
6.1 Overview.....	12	8.7 Glossary.....	43
6.2 Functional Block Diagram.....	13	<b>9 Revision History</b> .....	<b>43</b>
6.3 Feature Description.....	14	<b>10 Mechanical, Packaging, and Orderable Information</b> .....	<b>43</b>
6.4 Device Functional Modes.....	23		

## 4 Pin Configuration and Functions



Connect the exposed pad to AGND and PGND on the PCB.

**Figure 4-1. 19-Pin VQFN RGY Package (Top View)**

**Table 4-1. Pin Functions**

PIN		TYPE <sup>(1)</sup>	DESCRIPTION
NO.	NAME		
1	ISET	I/O	Dynamic current setting pin for the constant-current operation
2	RT	I	Frequency programming pin. A resistor from RT to AGND sets the oscillator frequency between 100kHz and 2.2MHz and DRSS disabled. A resistor from RT to VCC sets the oscillator frequency between 100kHz and 2.2MHz and DRSS enabled.
3	COMP	O	Transconductance error amplifier output. Connect the compensation network from COMP to AGND.
4	FB	I	Connect FB to VCC during initial power on to set the output voltage to pre-programmed fixed 12V. Connect FB to AGND during initial power on to set the output voltage to pre-programmed fixed 5V. Alternatively, install a resistor divider from VOUT to AGND to set the output voltage setpoint between 0.8V and 41V. The FB regulation voltage is 0.8V.
5	AGND	G	Analog ground connection. Ground return for the internal voltage reference and analog circuits.
6	IMON/ILIM	O	Current monitor and current limit programming pin
7	VCC	P	VCC bias supply pin. Connect a ceramic capacitor between VCC and PGND.
8	PGND	G	Power ground connection pin for low-side MOSFET gate driver.
9	LO	P	Low-side power MOSFET gate driver output.
10	VIN	P	Supply voltage input source for the VCC regulator.
11	HO	P	High-side power MOSFET gate driver output.
12	SW	P	Switching node of the buck regulator and high-side gate driver return. Connect to the bootstrap capacitor, the source terminal of the high-side MOSFET, and the drain terminal of the low-side MOSFET.
13	CBOOT	P	High-side driver supply for bootstrap gate drive.
14	BIAS	P	Optional supply voltage input source for VCC regulator. This input takes over if $V_{BIAS} > 9V$ (typical).
15	PGOOD	O	Power-good pin. An open-collector output that goes low if VOUT is outside the specified regulation window.

**Table 4-1. Pin Functions (continued)**

PIN		TYPE <sup>(1)</sup>	DESCRIPTION
NO.	NAME		
16	FPWM/SYNC	I	Connect FPWM/SYNC to VCC to enable forced PWM (FPWM) mode with continuous conduction at light loads. Connect FPWM/SYNC to AGND to operate the LM25190 in diode emulation mode. FPWM/SYNC can also be used as a synchronization input to synchronize the internal oscillator to an external clock signal.
17	EN	I	An active-high precision input with rising threshold of 1V and hysteresis voltage of 100mV. If the EN voltage is less than 0.55V, the LM25190 is in shutdown mode.
18	ISNS+	I	Current sense amplifier input. Connect this pin to the inductor side of the external current sense resistor using a low-current Kelvin connection.
19	VOUT	I	Output voltage sense and the current sense amplifier input. Connect VOUT to the output side of the current sense resistor.

(1) P = Power, G = Ground, I = Input, O = Output

## 5 Specifications

### 5.1 Absolute Maximum Ratings

Over the recommended operating junction temperature range of  $-40^{\circ}\text{C}$  to  $150^{\circ}\text{C}$  (unless otherwise noted). <sup>(1)</sup>

		MIN	MAX	UNIT
Input voltage	VIN to AGND	-0.3	45	V
Input voltage	SW to AGND	-0.3	45	V
Input voltage	SW to AGND, transient < 20ns	-5		V
Input voltage	CBOOT to SW	-0.3	10	V
Input voltage	CBOOT to AGND	-0.3	53	V
Input voltage	EN to AGND	-0.3	45	V
Input voltage	BIAS to AGND	-0.3	30	V
Input voltage	VCC, FB, PGOOD, FPWM/SYNC, RT to AGND	-0.3	8	V
Input voltage	ISET, IMON/ILIM to AGND	-0.3	5.5	V
Input voltage	VOUT, ISNS+ to AGND	-0.3	45	V
Input voltage	VOUT to ISNS+	-0.3	0.3	V
Output voltage	HO to SW, transient < 20ns	-5		V
Output voltage	LO to PGND, transient < 20ns	-1.5		V
Operating junction temperature, $T_J$		-40	150	$^{\circ}\text{C}$
Storage temperature, $T_{stg}$		-55	150	$^{\circ}\text{C}$

- (1) Operation outside the Absolute Maximum Ratings may cause permanent device damage. Absolute Maximum Ratings do not imply functional operation of the device at these or any other conditions beyond those listed under Recommended Operating Conditions. If used outside the Recommended Operating Conditions but within the Absolute Maximum Ratings, the device may not be fully functional, and this may affect device reliability, functionality, performance, and shorten the device lifetime.

### 5.2 ESD Ratings

			VALUE	UNIT
$V_{(ESD)}$	Electrostatic discharge	Human-body model (HBM), per ANSI/ESDA/ JEDEC JS-001 <sup>(1)</sup>	$\pm 2000$	V
		Charged-device model (CDM), per ANSI/ESDA/ JEDEC JS-002 <sup>(2)</sup>	$\pm 750$	

- (1) JEDEC document JEP155 states that 500V HBM allows safe manufacturing with a standard ESD control process.  
 (2) JEDEC document JEP157 states that 250V CDM allows safe manufacturing with a standard ESD control process.

### 5.3 Recommended Operating Conditions

Over the operating junction temperature range of  $-40^{\circ}\text{C}$  to  $150^{\circ}\text{C}$  (unless otherwise noted). <sup>(1)</sup>

		MIN	NOM	MAX	UNIT
$V_{IN}$	Input supply voltage range	5		42	V
$V_{OUT}$	Output voltage range	0.8		41	V
Pin Voltage	PGOOD, FB, FPWM/SYNC, RT	0		8	V
Pin Voltage	COMP, ISET, IMON	0		5.25	V
Pin Voltage	EN	0		42	V
Pin Voltage	BIAS	0		28	V
Pin Voltage	VOUT, ISNS+	0		41	V
$T_J$	Operating junction temperature	-40		150	$^{\circ}\text{C}$

- (1) Recommended operating conditions are conditions under which the device is intended to be functional. For specifications and test conditions, see the Electrical Characteristics.

## 5.4 Thermal Information

THERMAL METRIC <sup>(1)</sup>		LM25190	UNIT
		RGY (VQFN)	
		19 PINS	
R <sub>θJA</sub>	Junction-to-ambient thermal resistance	44.8	°C/W
R <sub>θJC(top)</sub>	Junction-to-case (top) thermal resistance	40.1	°C/W
R <sub>θJB</sub>	Junction-to-board thermal resistance	21.1	°C/W
ψ <sub>JT</sub>	Junction-to-top characterization parameter	0.9	°C/W
ψ <sub>JB</sub>	Junction-to-board characterization parameter	21.0	°C/W
R <sub>θJC(bot)</sub>	Junction-to-case (bottom) thermal resistance	6.0	°C/W

(1) For more information about traditional and new thermal metrics, see the [Semiconductor and IC Package Thermal Metrics](#) application note.

## 5.5 Electrical Characteristics

T<sub>J</sub> = –40°C to 150°C. Typical values are at T<sub>J</sub> = 25°C, V<sub>IN</sub> = 12V, and EN tied to VIN (unless otherwise noted).

PARAMETER		TEST CONDITIONS	MIN	TYP	MAX	UNIT
<b>SUPPLY (VIN)</b>						
I <sub>Q-SD</sub>	VIN shutdown current	V <sub>EN</sub> = 0V		2.3	4.5	μA
I <sub>Q-SBY</sub>	VIN standby current	Non-switching, 0.5V ≤ V <sub>EN</sub> ≤ 1V		100		μA
I <sub>SLEEP1</sub>	Sleep current, 5V	V <sub>IN</sub> = 24V, V <sub>VOUT</sub> = V <sub>BIAS</sub> = 5V, in sleep mode, V <sub>FPWM/SYNC</sub> = AGND, ISET floating		15	30	μA
I <sub>SLEEP2</sub>	Sleep current, 12V	V <sub>IN</sub> = 24V, V <sub>VOUT</sub> = V <sub>BIAS</sub> = 12V, in sleep mode, V <sub>FPWM/SYNC</sub> = AGND, ISET floating		20	35	μA
<b>ENABLE (EN)</b>						
V <sub>SBY-TH</sub>	Shutdown-to-standby threshold	V <sub>EN</sub> rising		0.55		V
V <sub>EN-TH</sub>	Enable voltage rising threshold	V <sub>EN</sub> rising, enable switching	0.95	1.0	1.05	V
V <sub>EN-HYS</sub>	Enable hysteresis voltage			100		mV
<b>INTERNAL LDO (VCC)</b>						
V <sub>VCC-REG</sub>	VCC regulation voltage	I <sub>VCC</sub> = 0mA to 110mA	7.125	7.5	7.875	V
V <sub>VCC-UVLO</sub>	VCC UVLO rising threshold		4.65	4.8	4.95	V
V <sub>VCC-HYS</sub>	VCC UVLO hysteresis			425		mV
I <sub>VCC-LIM</sub>	Internal LDO short-circuit current limit			220		mA
<b>EXTERNAL BIAS (BIAS)</b>						
V <sub>BIAS-TH</sub>	V <sub>IN</sub> to V <sub>BIAS</sub> switchover rising threshold		8.55	9	9.45	V
V <sub>BIAS-HYS</sub>	V <sub>IN</sub> to V <sub>BIAS</sub> switchover hysteresis			400		mV
<b>REFERENCE VOLTAGE</b>						
V <sub>REF-V</sub>	Regulated FB voltage	V <sub>IMON</sub> = 0V	792	800	808	mV
V <sub>REF-I</sub>	Current loop reference voltage	V <sub>FB</sub> = 0V	0.99	1	1.01	V
<b>OUTPUT VOLTAGE (VOUT)</b>						
V <sub>OUT-5V</sub>	5V output voltage setpoint	FB tied to AGND	4.95	5.0	5.05	V
V <sub>OUT-12V</sub>	12V output voltage setpoint	FB tied to VCC, V <sub>IN</sub> = 24V	11.88	12	12.12	V
<b>ERROR AMPLIFIER (COMP)</b>						
g <sub>m-VEA</sub>	Voltage loop EA transconductance	ΔV <sub>FB</sub> = 100mV		1000		μS
g <sub>m-IEA</sub>	Current loop EA transconductance	ΔV <sub>IMON</sub> = 100mV		1000		μS
I <sub>FB</sub>	Error amplifier input bias current				75	nA
I <sub>COMP-SRC</sub>	EA source current	V <sub>COMP</sub> = 1V		120		μA
I <sub>COMP-SINK</sub>	EA sink current	V <sub>COMP</sub> = 1V		120		μA
<b>OUTPUT CURRENT MONITOR (IMON/ILIM)</b>						
g <sub>m-MON</sub>	Monitor amplifier gain from V <sub>CS</sub>	V <sub>CS</sub> = 40mV	1.94	2	2.06	μA/mV
I <sub>OFFSET</sub>	Monitor amplifier offset current	V <sub>CS</sub> = 0mV	22.5	25	27.5	μA
<b>CURRENT SETTING (ISET)</b>						
I <sub>ISET</sub>	ISET source current		9	10	11	μA

## 5.5 Electrical Characteristics (continued)

$T_J = -40^{\circ}\text{C}$  to  $150^{\circ}\text{C}$ . Typical values are at  $T_J = 25^{\circ}\text{C}$ ,  $V_{IN} = 12\text{V}$ , and EN tied to VIN (unless otherwise noted).

PARAMETER		TEST CONDITIONS	MIN	TYP	MAX	UNIT
<b>FORCED PWM MODE (FPWM/SYNC)</b>						
$V_{ZC-SW}$	Zero-cross threshold	SW-PGND threshold		-5.5		mV
<b>SWITCHING FREQUENCY</b>						
$V_{RT}$	RT pin regulation voltage	$10\text{k}\Omega < R_{RT} < 242\text{k}\Omega$		1		V
$F_{SW1}$	Switching frequency 1	$V_{IN} = 12\text{V}$ , $R_{RT} = 242\text{k}\Omega$ to AGND	90	100	110	kHz
$F_{SW2}$	Switching frequency 2	$V_{IN} = 12\text{V}$ , $R_{RT} = 10\text{k}\Omega$ to AGND	2.0	2.2	2.4	MHz
$V_{SLOPE}$	Slope compensation ramp amplitude	Referenced to ISNS+ to VOUT input		45		mV
$t_{ON-MIN}$	Minimum on-time			26	50	ns
$t_{OFF-MIN}$	Minimum off-time			80	125	ns
<b>POWER GOOD (PGOOD)</b>						
$V_{PG-UV}$	Power-Good UV trip level	Falling with respect to the regulated voltage	90%	92%	94%	
$V_{PG-OV}$	Power-Good OV trip level	Rising with respect to the regulated voltage	108%	110%	112%	
$V_{PG-UV-HYST}$	Power-Good UV hysteresis			3.7%		
$V_{PG-OV-HYST}$	Power-Good OV hysteresis			3.7%		
$V_{PG-OL}$	PG voltage	Open collector, $I_{PG} = 4\text{mA}$			0.8	V
<b>OVERVOLTAGE PROTECTION</b>						
$V_{OVTH-RISING}$	Overvoltage threshold	Rising with respect to regulated voltage	108%	110%	112%	
$V_{OVTH-HYST}$	Overvoltage threshold hysteresis			3.7%		
<b>STARTUP (Soft Start)</b>						
$t_{SS-INT}$	Internal fixed soft-start time		1.9	2.75	3.8	ms
<b>BOOT CIRCUIT</b>						
$V_{BOOT-DROP}$	Internal diode forward drop	$I_{CBOOT} = 20\text{mA}$ , VCC to CBOOT		0.8	1	V
$I_{BOOT}$	CBOOT to SW quiescent current, not switching	$V_{EN} = 5\text{V}$ , $V_{CBOOT-SW} = 7.5\text{V}$			25	$\mu\text{A}$
$V_{BOOT-SW-UV-F}$	CBOOT to SW UVLO falling threshold	$V_{CBOOT-SW}$ falling	2.75	3.1	3.75	V
$V_{BOOT-SW-UV-HYS}$	CBOOT to SW UVLO hysteresis			0.3		V
<b>HIGH-SIDE GATE DRIVER (HO)</b>						
$V_{HO-HIGH}$	HO high-state output voltage	$I_{HO} = -100\text{mA}$ , $V_{HO-HIGH} = V_{CBOOT} - V_{HO}$		300		mV
$V_{HO-LOW}$	HO low-state output voltage	$I_{HO} = 100\text{mA}$		75		mV
$t_{HO-RISE}$	HO rise time (10% to 90%)	$C_{LOAD} = 2.7\text{nF}$		20		ns
$t_{HO-FALL}$	HO fall time (90% to 10%)	$C_{LOAD} = 2.7\text{nF}$		8		ns
<b>LOW-SIDE GATE DRIVER (LO)</b>						
$V_{LO-HIGH}$	LO high-state output voltage	$I_{LO} = -100\text{mA}$		300		mV
$V_{LO-LOW}$	LO low-state output voltage	$I_{LO} = 100\text{mA}$		75		mV
$t_{LO-RISE}$	LO rise time (10% to 90%)	$C_{LOAD} = 2.7\text{nF}$		20		ns
$t_{LO-FALL}$	LO fall time (90% to 10%)	$C_{LOAD} = 2.7\text{nF}$		8		ns
<b>ADAPTIVE DEADTIME CONTROL</b>						
$t_{DEAD1}$	HO off to LO on deadtime			21		ns
$t_{DEAD2}$	LO off to HO on deadtime			21		ns
<b>OVERCURRENT PROTECTION</b>						
$V_{CS-TH}$	Current limit threshold	Measured from ISNS+ to VOUT	54	60	68	mV
$V_{CS-TH-MIN}$	Minimum peak current limit threshold	Measured from ISNS+ to VOUT		12		mV
$A_{CS}$	CS amplifier gain		9.5	10	10.6	V/V
$V_{CS-NEG}$	CS negative voltage threshold			-30		mV
<b>THERMAL SHUTDOWN</b>						
$T_{J-SD}$	Thermal shutdown threshold <sup>(1)</sup>	Temperature rising		175		$^{\circ}\text{C}$
$T_{J-HYS}$	Thermal shutdown hysteresis <sup>(1)</sup>			15		$^{\circ}\text{C}$

(1) Specified by design. Not production tested.

## 5.6 Typical Characteristics

$V_{IN} = 12V$ , unless otherwise specified

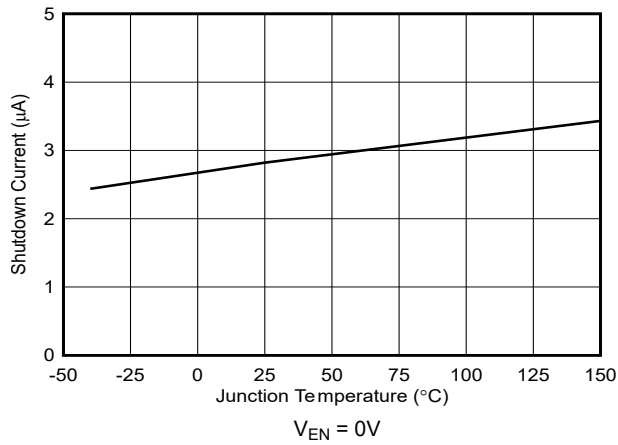


**Figure 5-1. Shutdown Current vs Temperature**

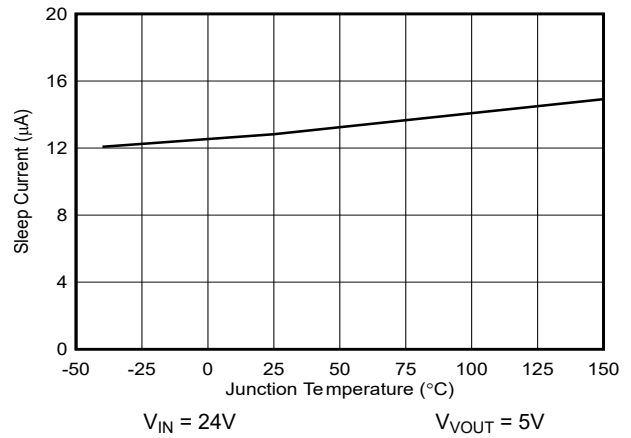


**Figure 5-2. Sleep1 Current vs Temperature**

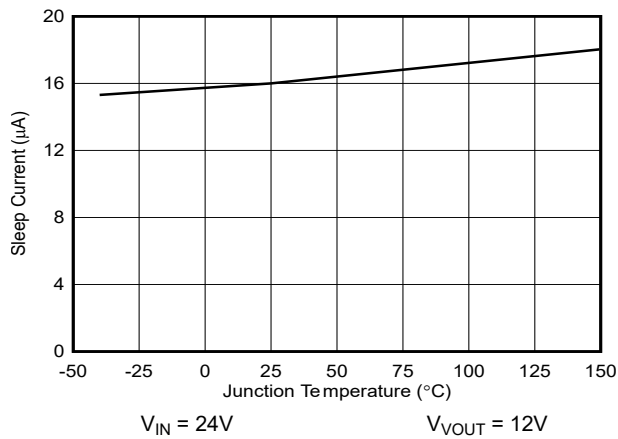


**Figure 5-3. Sleep2 Current vs Temperature**

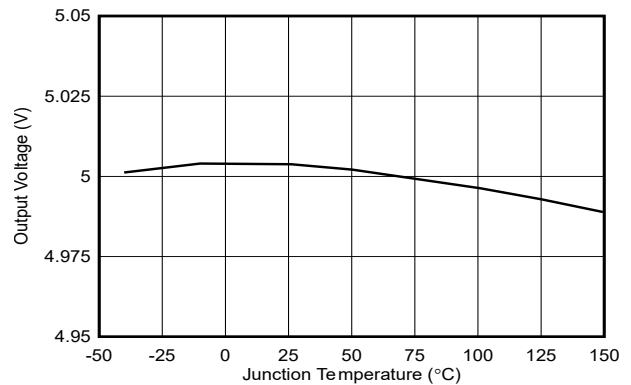


**Figure 5-4. Fixed 5V Output Voltage vs Temperature**

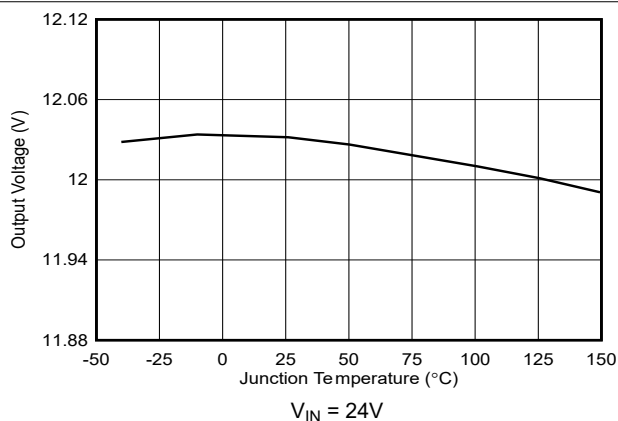


**Figure 5-5. Fixed 12V Output Voltage vs Temperature**

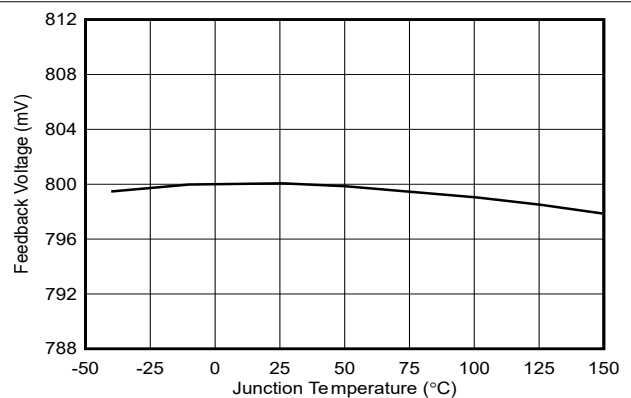


**Figure 5-6. Feedback Voltage vs Temperature**

## 5.6 Typical Characteristics (continued)

$V_{IN} = 12V$ , unless otherwise specified

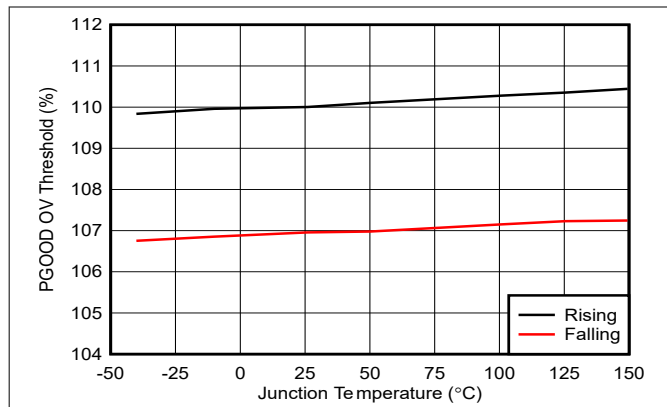


Figure 5-7. PG OV Thresholds vs Temperature

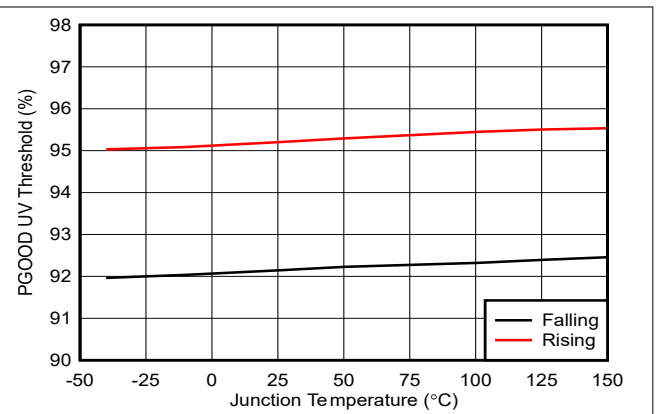


Figure 5-8. PG UV Thresholds vs Temperature

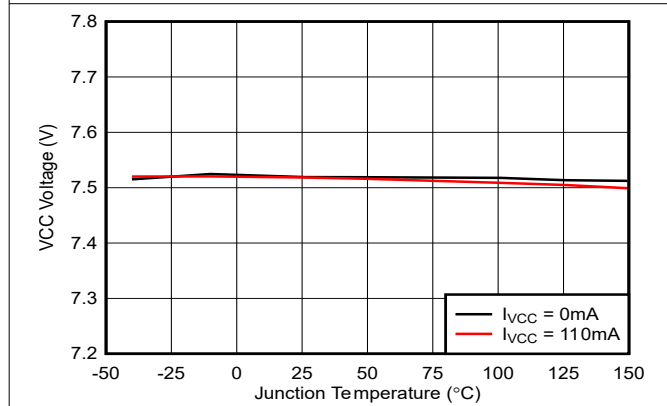


Figure 5-9. VCC Regulation Voltage vs Temperature

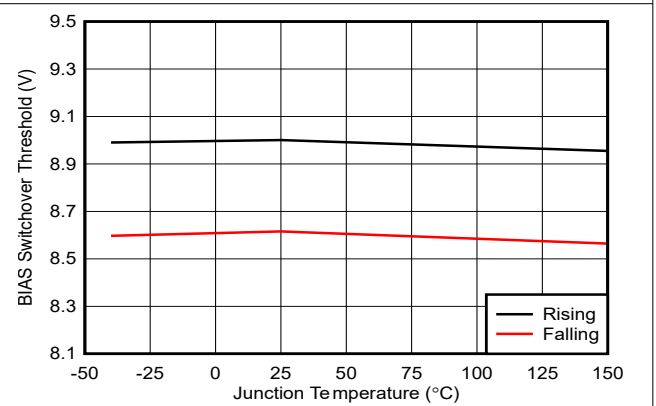


Figure 5-10. BIAS Switchover Thresholds vs Temperature

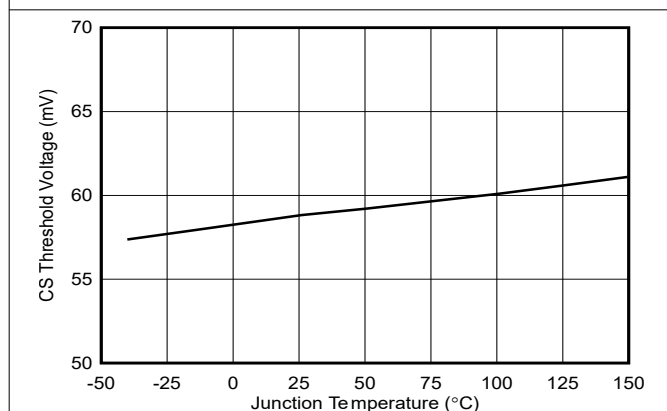


Figure 5-11. Current Sense (CS) Threshold vs Temperature

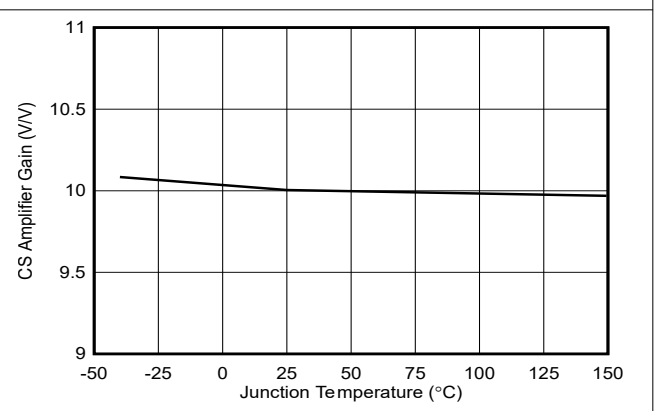


Figure 5-12. Current Sense (CS) Amplifier Gain vs Temperature

## 5.6 Typical Characteristics (continued)

$V_{IN} = 12V$ , unless otherwise specified

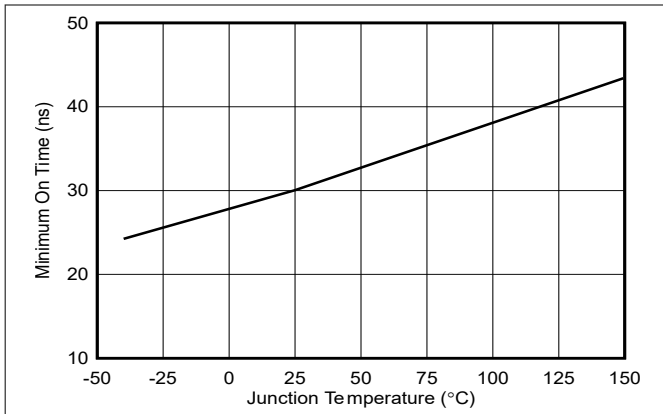


Figure 5-13. Minimum On Time (HO) vs Temperature

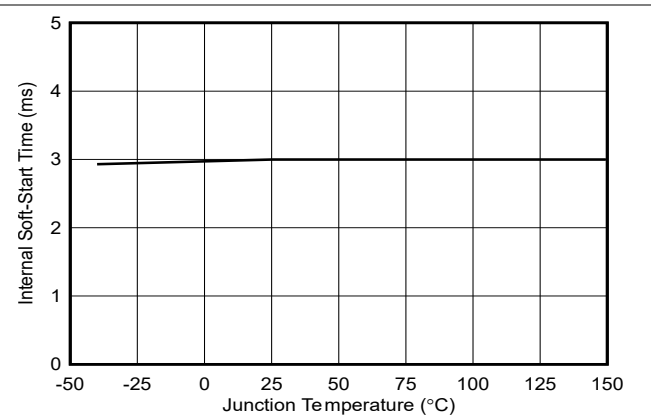


Figure 5-14. Soft-Start Time vs Temperature

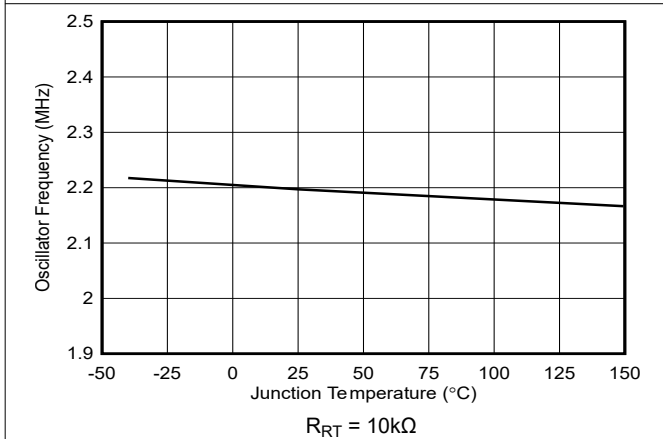


Figure 5-15. Switching Frequency vs Temperature

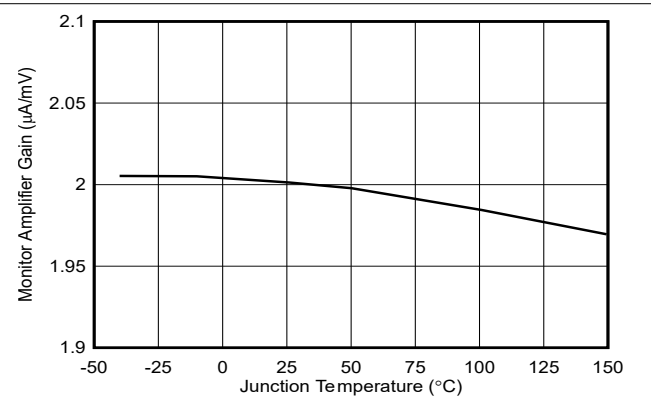


Figure 5-16. Monitor Amplifier Gain vs Temperature

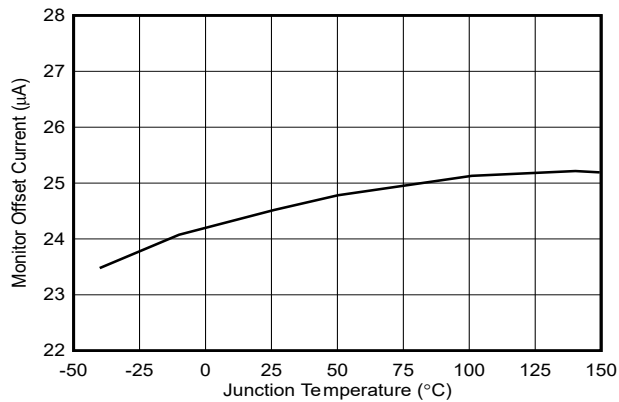


Figure 5-17. Monitor Offset Current vs Temperature

## 6 Detailed Description

### 6.1 Overview

The LM25190 is a switching DC/DC controller that features all of the functions necessary to implement a high-efficiency constant-current constant-voltage synchronous buck regulator operating over a wide input voltage range from 5V to 42V. The LM25190 is configured to provide a fixed 5V or 12V output, or an adjustable output from 0.8V to 41V. This easy-to-use controller integrates high-side and low-side MOSFET gate drivers capable of sourcing and sinking peak currents of 1.5A and 2.5A, respectively. Adaptive dead-time control is designed to minimize body diode conduction during switching transitions.

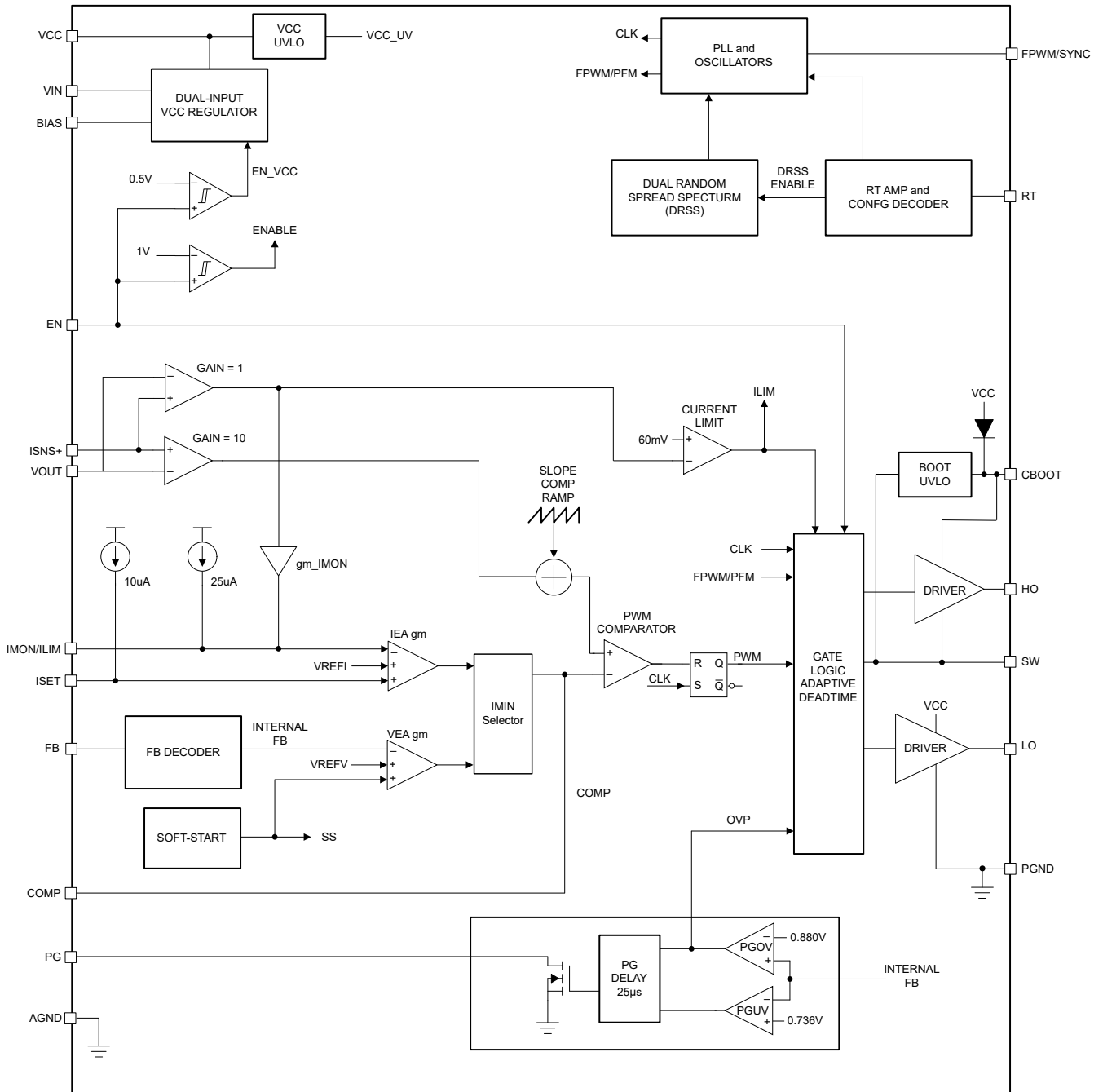
The current-mode control architecture using a shunt resistor current sensing provides inherent line feedforward, cycle-by-cycle peak current limiting, and easy loop compensation. Current-mode control also supports a wide duty cycle range for high input voltage and low-dropout applications as well as when application require a high step-down conversion ratio (for example, 10-to-1). The oscillator frequency is user-programmable between 100kHz to 2.2MHz, and the frequency can be synchronized as high as 2.5MHz by applying an external clock to the FPWM/SYNC pin.

An external bias supply can be connected to BIAS to maximize efficiency in high input voltage applications. A user-selectable diode emulation feature enables discontinuous conduction mode (DCM) operation to further improve efficiency and reduce power dissipation during light-load conditions. Fault protection features include current limiting, hiccup mode over-load protection, thermal shutdown, UVLO, and remote shutdown capability.

The LM25190 incorporates features to simplify the compliance with various EMI standards, for example CISPR 11 and CISPR 32 Class B requirements. [DRSS](#) techniques reduce the peak harmonic EMI signature.

The LM25190 is provided in a custom 19-pin VQFN package with an exposed pad to aid in thermal dissipation.

## 6.2 Functional Block Diagram



## 6.3 Feature Description

### 6.3.1 Input Voltage Range ( $V_{IN}$ )

The LM25190 operational input voltage range is from 5V to 42V. The device is intended for step-down conversions from 12V and 24V supply rails. The LM25190 uses an internal LDO to provide a 7.5V VCC bias rail for the gate drive and control circuits (assuming the input voltage is higher than 7.5V with additional voltage margin necessary for the subregulator dropout specification).

In high input voltage applications, take extra care to make sure that the VIN and SW pins do not exceed the absolute maximum voltage rating of 47V during line or load transient events. Voltage excursions that exceed the applicable voltage specifications can damage the device.

### 6.3.2 High-Voltage Bias Supply Regulator (VCC, BIAS)

The LM25190 contains an internal high-voltage VCC bias regulator that provides the bias supply for the PWM controller and the gate drivers for the external MOSFETs. The VCC voltage is regulated at 7.5V to support the standard-level MOSFETs as well as the logic-level MOSFETs. The input voltage pin (VIN) can be connected directly to an input voltage source up to 42V. However, when the input voltage is below the VCC setpoint level, the VCC voltage tracks  $V_{IN}$  minus a small voltage drop.

The VCC regulator output current limit is 135mA (minimum). At power up, the controller sources current into the capacitor connected at the VCC pin. When the VCC voltage exceeds 4.8V and the EN pin is connected to a voltage greater than 1V, the soft-start sequence begins. The output remains active unless the VCC voltage falls below the VCC UVLO falling threshold of 4.375V (typical) or EN is switched to a low state. Connect a ceramic capacitor from VCC to PGND. The recommended range of the VCC capacitor is from 2.2 $\mu$ F to 10 $\mu$ F.

The VCC regulator is a dual-input regulator which uses BIAS pin as the other input in addition to the VIN pin. A lower voltage supply such as the buck output (VOUT) or other applicable system rails can be tied to BIAS to reduce the power dissipation of the internal VCC regulator. The VCC regulator switches over to use BIAS voltage as the input when rising across 9V (typical). The switchover voltage hysteresis is 400mV. When using BIAS as the supply, VIN voltage must be greater than VCC voltage during all conditions to avoid damage to the controller. Tie BIAS to PGND if unused. The operational maximum voltage of BIAS is 28V.

### 6.3.3 Precision Enable (EN)

The EN pin can be connected to a voltage as high as 42V. The LM25190 has a precision enable. When the EN voltage is greater than 1V, controller switching is enabled. If the EN pin is pulled below 0.55V, the LM25190 is in shutdown with an  $I_Q$  of 2.3 $\mu$ A (typical) current consumption from  $V_{IN}$ . When the enable voltage is between 0.55V and 1V, the LM25190 is in standby mode with the VCC regulator active but the controller is not switching. In standby mode, the non-switching input quiescent current is 100 $\mu$ A typical. The LM25190 is enabled with a voltage greater than 1.0V. Many applications benefit from using a resistor divider  $R_{ENT}$  and  $R_{ENB}$  to establish a precision UVLO level from  $V_{SUPPLY}$  (supply voltage of power stage tied to the VIN pin). TI does not recommend leaving the EN pin floating.

### 6.3.4 Power-Good Monitor (PGOOD)

The LM25190 includes an output voltage monitoring signal for  $V_{OUT}$  to simplify sequencing and supervision. The power-good signal is used for start-up sequencing of downstream converters, fault protection, and output monitoring. The power-good output (PGOOD) switches to a high impedance open-drain state when the output voltage is in regulation. The PGOOD switches low when the output voltage drops below the lower power-good threshold (92% typical) or rises above the upper power-good threshold (110% typical). If the upper PG threshold is exceeded, the high-side switch is turned off immediately and the low-side switch is turn on to prevent overvoltage and discharge the output. A 25 $\mu$ s deglitch filter prevents false tripping of the power-good signal during transients. TI recommends a pullup resistor of 100k $\Omega$  (typical) from PGOOD to the relevant logic rail. PGOOD is asserted low during soft start and when the buck regulator is disabled.

### 6.3.5 Switching Frequency (RT)

Program the LM25190 oscillator with a resistor from RT to AGND or VCC to set an oscillator frequency from 100kHz and 2.2MHz. If the resistor is connected between RT and VCC during initial power on, the dual random

spread spectrum (DRSS) is on. If the resistor is connected between RT and AGND during initial power on, the DRSS is off. See more details about DRSS in [Section 6.3.7](#). Calculate the RT resistance for a given switching frequency using [Equation 1](#).

$$R_{RT} [\text{k}\Omega] = \frac{10^6}{f_{sw} [\text{kHz}]^{41}} - 59 \quad (1)$$

### 6.3.6 Low Dropout Mode

For extended minimum input voltage, LM25190 enters the low dropout (LDO) mode if the required duty cycle is greater than the maximum duty cycle that is limited by the minimum off time. During the LDO mode, the LM25190 extends the on-time pulse until the PWM latch is reset by the current sense ramp exceeding the controller compensation voltage. The LM25190 skips up to 15  $t_{OFF}$  cycles to allow the controller to extend the duty cycle. [Figure 6-1](#) shows the normal PWM mode to LDO mode transition.

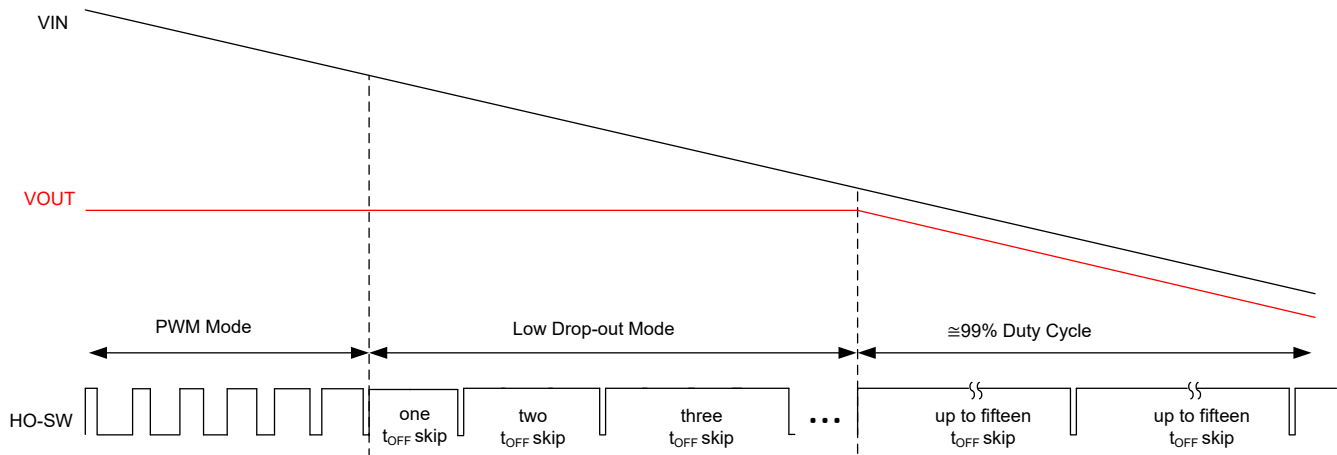


**Figure 6-1. PWM to LDO Mode Transition**

The approximate input voltage level at which this occurs is given by [Equation 2](#).

$$V_{IN(MIN)} = V_{OUT} \times \frac{t_{SW}}{t_{SW} - t_{OFF(MIN)}} \quad (2)$$

where

- $t_{SW}$  is the extended switching period.
- $t_{OFF(MIN)}$  is the minimum off time of 80ns (typical).

### 6.3.7 Dual Random Spread Spectrum (DRSS)

The LM25190 provides a digital spread spectrum, which reduces the EMI of the power supply over a wide frequency range. DRSS combines a low-frequency triangular modulation profile with a high frequency cycle-by-cycle random modulation profile. The low-frequency triangular modulation improves performance in lower radio-frequency bands, while the high-frequency random modulation improves performance in higher radio frequency bands.

Spread spectrum works by converting a narrowband signal into a wideband signal that spreads the energy over multiple frequencies. Because industry standards require different EMI receiver resolution bandwidth (RBW) settings for different frequency bands, the RBW has an impact on the spread spectrum performance. DRSS is able to simultaneously improve the EMI performance in the low and high RBWs using the low-frequency triangular modulation profile and at high frequency cycle-by-cycle random modulation, respectively. DRSS can reduce conducted emissions up to 15dB $\mu$ V in the low-frequency band (150kHz to 30MHz) and 5dB $\mu$ V in the high-frequency band (30MHz to 108MHz).

To enable DRSS, connect RT to VCC through a resistor during initial power on. The resistor is still used to set the switching frequency with the same equation in Equation 1.

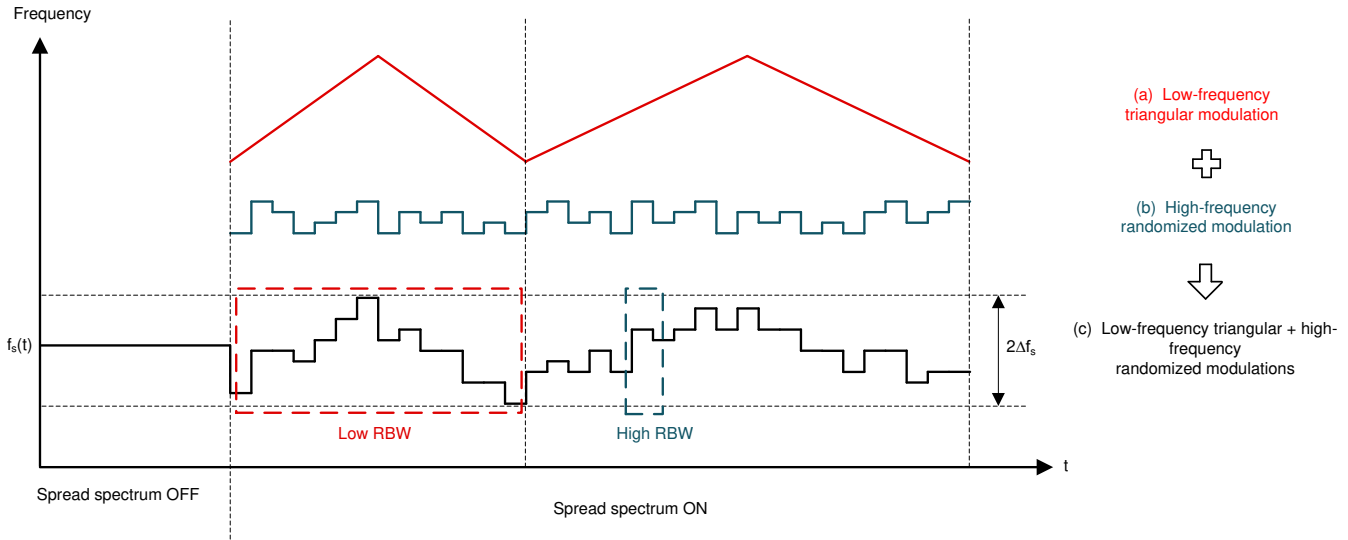


**Figure 6-2. Dual Random Spread Spectrum Implementation**

### 6.3.8 Soft Start

The LM25190 has an internal 2.75ms (typical) soft-start timer. The soft-start feature allows the regulator to gradually reach the steady-state operating point, thus reducing start-up stresses and surges.

### 6.3.9 Output Voltage Setpoint (FB)

The LM25190 regulator output can be independently configured for one of two fixed output voltages without external feedback resistors, or adjusted to a desired voltage using an external resistor divider. Set the output to 5V by connecting FB to AGND during initial power on. Set the output to 12V by connecting FB to VCC during initial power on. See Table 6-1.

**Table 6-1. Output Regulation Targets**

FB SELECTION	V <sub>OUT</sub> SETPOINT
FB = VCC	12V
FB = AGND	5V
FB = FB resistors	Adjustable

The configuration settings are latched and cannot be changed until the LM25190 is powered down (with the VCC voltage decreasing below the falling UVLO threshold) and then powered up again (VCC rises above 4.8V typical). Alternatively, the output regulation target can be adjusted during operation by connecting external feedback divider resistors whose parallel resistance is greater than 5.0kΩ (see Equation 3).

$$5 \text{ k}\Omega < \frac{R_{FBT} \times R_{FBB}}{R_{FBT} + R_{FBB}} \quad (3)$$

The output voltage adjustment range is between 0.8V and 41V. The regulation voltage at FB is 0.8V (V<sub>REF-V</sub>). Use Equation 4 to calculate the top and bottom feedback resistors, designated as R<sub>FBT</sub> and R<sub>FBB</sub>, respectively.

$$R_{FBT} = \left( \frac{V_{OUT}}{V_{REF}} - 1 \right) \times R_{FBB} \quad (4)$$

If low- $I_Q$  operation is required, take care when selecting the external feedback resistors. The current consumption of the external divider adds to the LM25190 sleep current (15 $\mu$ A typical). The divider current reflected to  $V_{IN}$  is scaled by the ratio of  $V_{OUT} / V_{IN}$ .

### 6.3.10 Minimum Controllable On Time

There are two limitations to the minimum output voltage adjustment range: the LM25190 voltage reference of 0.8V and the minimum controllable switch-node pulse width,  $t_{ON(min)}$ .

$t_{ON(min)}$  effectively limits the voltage step-down conversion ratio  $V_{OUT} / V_{IN}$  at a given switching frequency. For fixed-frequency PWM operation, the voltage conversion ratio must satisfy [Equation 5](#).

$$\frac{V_{OUT}}{V_{IN}} > t_{ON(min)} \times f_{SW} \quad (5)$$

where

- $t_{ON(min)}$  is 26ns (typical).
- $f_{SW}$  is the switching frequency.

If the desired voltage conversion ratio does not meet the above condition, the LM25190 transitions from fixed switching frequency operation to a pulse-skipping mode to maintain output voltage regulation. For example, if the desired output voltage is 5V with an input voltage of 24V and switching frequency of 2.1MHz, use [Equation 6](#), [Equation 7](#) to check the conversion ratio.

$$\frac{5V}{24V} > 26ns \times 2.1MHz \quad (6)$$

$$0.208 > 0.055 \quad (7)$$

For wide  $V_{IN}$  applications and low output voltages, an alternative is to reduce the LM25190 switching frequency to meet the requirement of [Equation 5](#).

### 6.3.11 Inductor Current Sense (ISNS+, VOUT)

[Figure 6-3](#) illustrates inductor current sensing using a shunt resistor. This configuration continuously monitors the inductor current to provide accurate overcurrent protection across the operating temperature range. For the best current sense accuracy and overcurrent protection, use a *low inductance*  $\pm 1\%$  tolerance shunt resistor between the inductor and the output, with a Kelvin connection to the LM25190 current sense amplifier.

If the peak voltage signal sensed from ISNS+ to VOUT exceeds the current limit threshold of 60mV, the current limit comparator immediately terminates the HO output for cycle-by-cycle peak current limiting. Calculate the shunt resistance using [Equation 8](#).

$$R_S = \frac{V_{CS-TH}}{I_{out(CL)} + \frac{\Delta I_L}{2}} \quad (8)$$

where

- $V_{CS-TH}$  is current sense threshold of 60mV.
- $I_{OUT(CL)}$  is the overcurrent setpoint that is set higher than the maximum load current to avoid tripping the overcurrent comparator during load transients.
- $\Delta I_L$  is the peak-to-peak inductor ripple current.

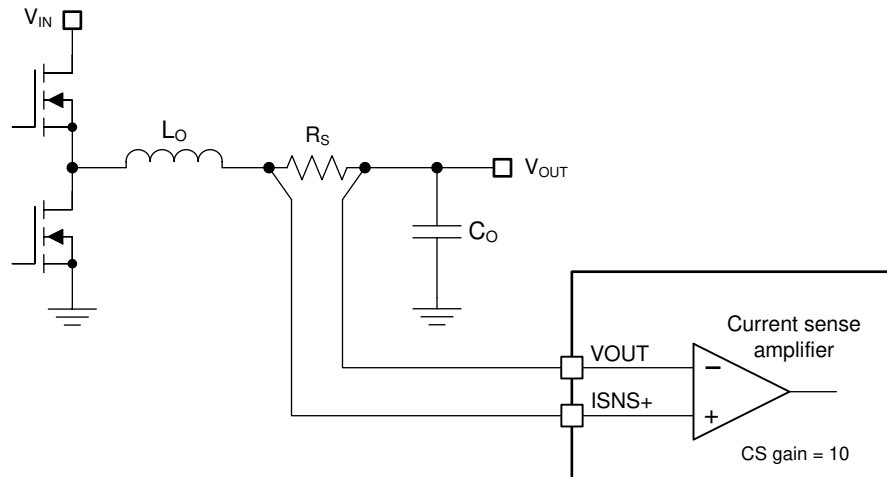


**Figure 6-3. Shunt Current Sensing Implementation**

The soft-start voltage is clamped 60mV above FB if the regulator is in an overcurrent condition or if the output is in UV (undervoltage) condition in CC mode operation. Eight overcurrent events must occur before the SS clamp is enabled. This requirement makes sure that SS can be pulled low during brief overcurrent events, preventing output voltage overshoot during recovery.

### 6.3.12 Voltage Loop Error Amplifier

In the voltage loop, the LM25190 has a high-gain transconductance amplifier that generates an error current proportional to the difference between the feedback voltage and an internal precision reference (0.8V). The transconductance of the amplifier is  $1000\mu S$ . The voltage loop error amplifier only takes control when the internal minimum function block IMIN selector selects the current from the voltage loop error amplifier. See [Section 6.3.14](#) for more details regarding the constant-current constant-voltage operation.

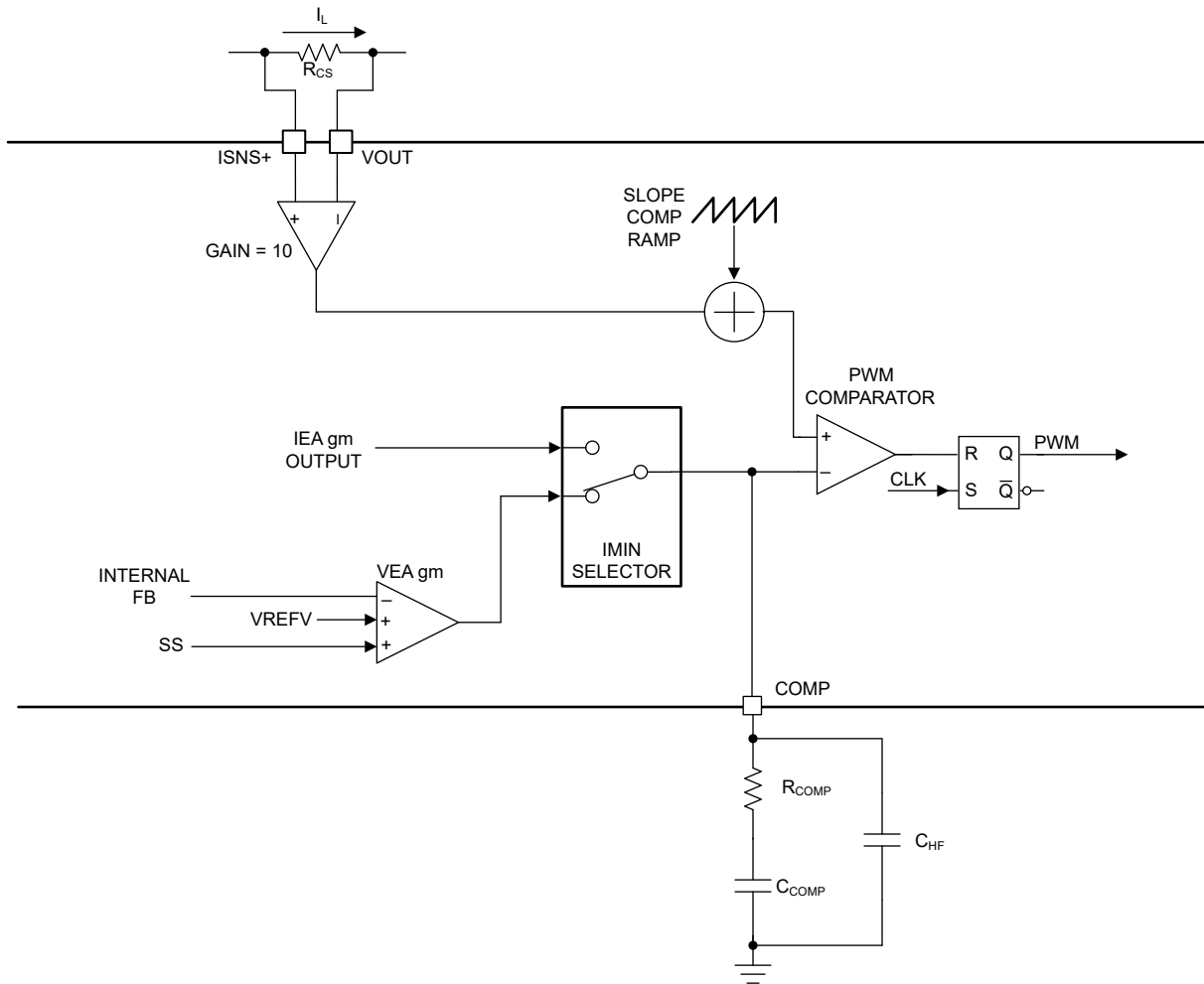


**Figure 6-4. Voltage Loop Functional Block Diagram**

A type-II compensation network is generally recommended for peak current-mode control.

### 6.3.13 Current Monitor, Programmable Current Limit, and Current Loop Error Amplifier (IMON/ILIM, ISET)

In the current loop, the LM25190 has a high-gain transconductance amplifier that generates an error current proportional to the difference between the IMON voltage and an internal precision reference (1V). The transconductance of the amplifier is  $1000\mu\text{S}$ . The current loop error amplifier only takes control when the internal minimum function block IMIN selector selects the current from the current loop error amplifier. See [Section 6.3.14](#) for more details regarding the constant-current constant-voltage operation.

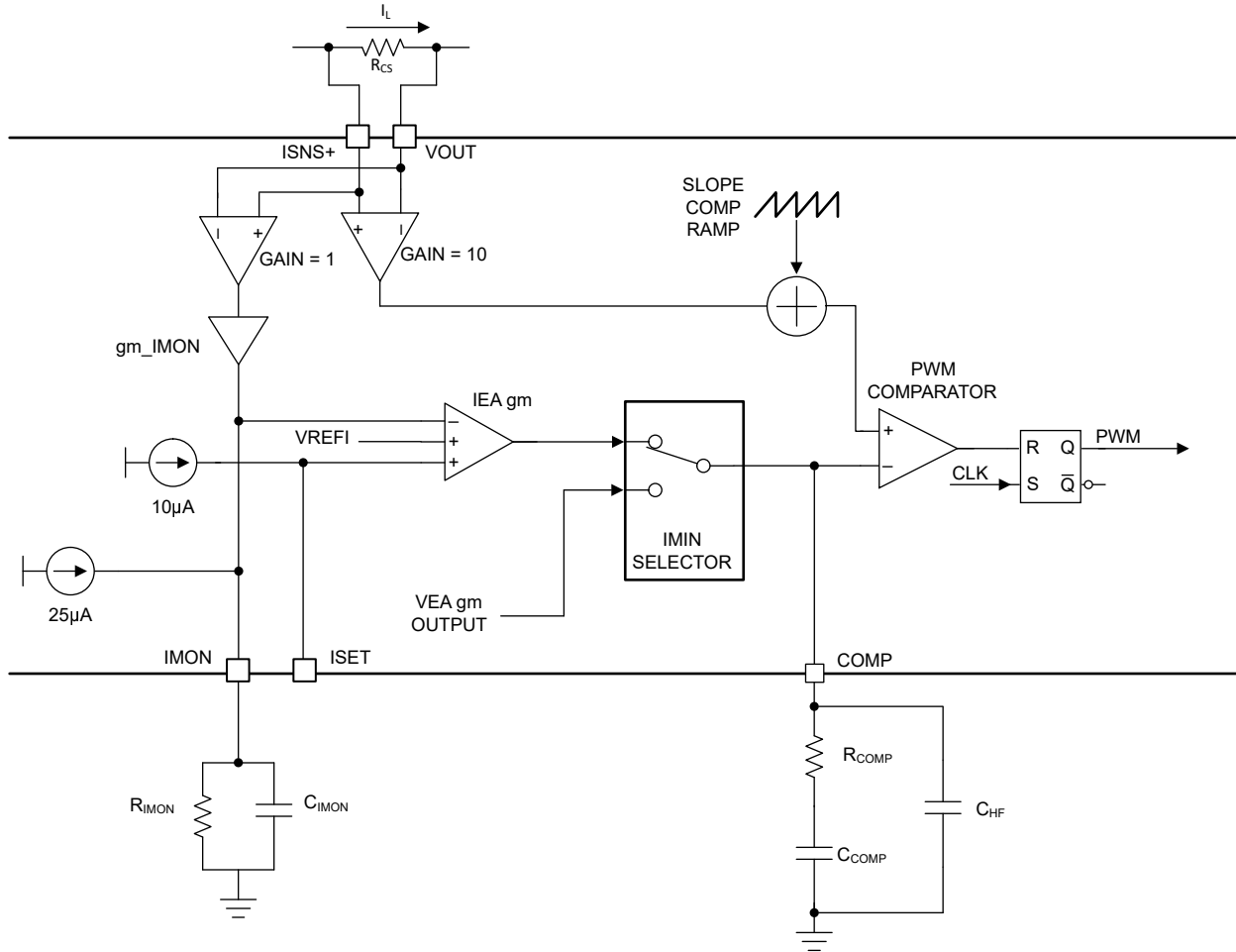


**Figure 6-5. Current Loop Functional Block Diagram**

The  $R_{IMON}$  is used to programmed the CC regulation target. The CC regulation target is usually defined to be smaller than the maximum current defined by the cycle-by-cycle peak current limit in *Inductor Current Sense (ISNS+, VOUT)*. The  $R_{IMON}$  is selected by Equation 9.

$$R_{IMON} = \frac{V_{refI}}{R_{CS} \times g_{m\_IMON} \times I_{CC} + I_{IMON\_offset}} \quad (9)$$

where

- $V_{refI}$  is 1V (typical).
- $R_{CS}$  is the current sensing resistance.
- $g_{m\_IMON}$  is the current monitor gain of 2µA/mV.
- $I_{CC}$  is the CC regulation target.
- $I_{IMON\_offset}$  is the IMON offset current of 25µA.

The  $C_{IMON}$  is used to form the RC filter with  $R_{IMON}$  and filter out the sensed inductor current ripple to the achieve average current regulation. The  $C_{IMON}$  also sets the response of the current loop. With  $R_{IMON}$  and  $C_{IMON}$  selected, IMON/ILIM multifunctional pin can be used as the current monitor when the regulator is operating in CV loop. The average inductor current can be read from IMON/ILIM voltage by using Equation 10.

$$I_{AVG} = \frac{\frac{V_{IMON}}{R_{IMON}} - I_{IMON\_offset}}{R_{CS} \times g_{m\_IMON}} \quad (10)$$

where  $V_{IMON}$  is the voltage on IMON/ILIM pin and  $I_{AVG}$  is the average inductor current. The DC offset current is introduced at IMON/ILIM pin to raise the no-load signal above the possible ground noise floor.

ISET can be used to dynamically program the CC regulation current. An external voltage forced at ISET can set the CC regulation current by Equation 11.

$$V_{ISET} = R_{IMON} \times (I_{CCset} \times R_{CS} \times g_{m_{IMON}} + I_{IMON\_offset}) \quad (11)$$

where  $I_{CCset}$  is the desired average current to be programmed by ISET. ISET is only functional when ISET voltage is smaller than  $V_{ref1}$  (1V typical). ISET has an internal current source of 10 $\mu$ A typical so ISET can be used with a capacitor at the pin to achieve the current soft start during CC transient such as super capacitor and battery charging conditions. Discharge this ISET capacitor externally if needed. Due to this internal current source, a resistor connected to ISET and AGND can also determine the voltage on ISET.

### 6.3.14 Dual Loop Architecture

In Section 6.3.12 and Section 6.3.13, the voltage loop and current loop operation have been discussed respectively. To have a seamless transition between CC and CV operation, a minimum function block called IMIN selector is used for the dual loop architecture. To operate LM25190 as normal buck in CV, ground IMON pin and leave ISET pin open.

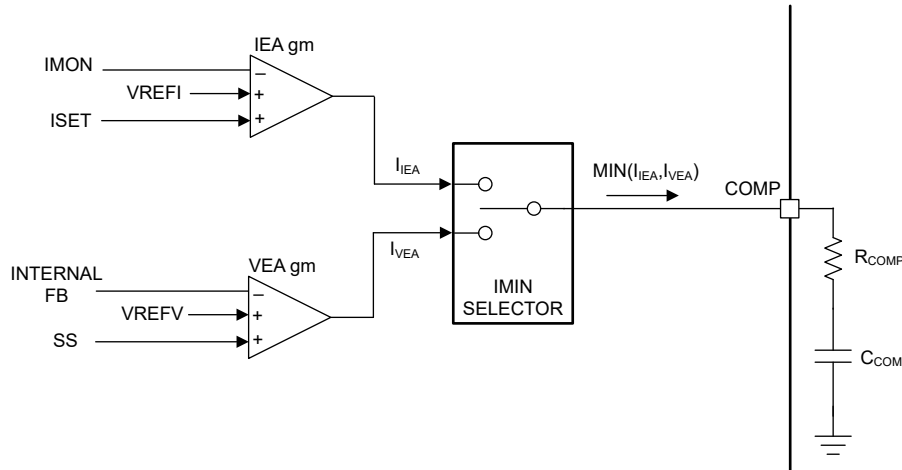


Figure 6-6. Dual Loop Architecture

### 6.3.15 PWM Comparator

The PWM comparator compares the sum of the amplified sensed inductor current and the slope compensation ramp with the COMP pin voltage minus a 0.6V internal offset, and terminates the present cycle if the sum of the amplified sensed inductor current and the slope compensation ramp is greater than the COMP pin voltage minus the 0.6V internal offset.

### 6.3.16 Slope Compensation

The LM25190 provides internal slope compensation for stable operation with peak current-mode control and a duty cycle greater than 50%. Calculate the buck inductance to provide a slope compensation contribution equal to one times the inductor downslope using Equation 12.

$$L_{O-IDEAL} [\mu\text{H}] = \frac{V_{OUT} [\text{V}] \times R_{CS} [\text{m}\Omega]}{45 \times f_{SW} [\text{MHz}]} \quad (12)$$

- A lower inductance value generally increases the peak-to-peak inductor current, which minimizes size and cost, and improves transient response at the cost of reduced light-load efficiency due to higher cores losses and peak currents.

- A higher inductance value generally decreases the peak-to-peak inductor current, reducing switch peak and RMS currents at the cost of requiring larger output capacitors to meet load-transient specifications.

### 6.3.17 Hiccup Mode Current Limiting

The LM25190 includes an internal hiccup-mode protection function. After 512 cycles of cycle-by-cycle peak current limiting occurs, the internal soft start is pulled low, the HO and LO driver outputs are disabled, and the 16384 counter is enabled. The 512-cycle counter is reset if four consecutive switching cycles occur without exceeding the current limit threshold. After the counter reaches 16384, the internal soft start is enabled and the output restarts.

### 6.3.18 High-Side and Low-Side Gate Drivers (HO, LO)

The LM25190 contains gate drivers and an associated high-side level shifter to drive the external N-channel power MOSFETs. The high-side gate driver works in conjunction with an internal bootstrap diode  $D_{BOOT}$  and bootstrap capacitor  $C_{BOOT}$ . During the conduction interval of the low-side MOSFET, the SW voltage is approximately 0V and CBOOT charges from VCC through the internal  $D_{BOOT}$ . TI recommends a 0.1 $\mu$ F ceramic capacitor connected with short traces between the CBOOT and SW pins.

The HO and LO outputs are controlled with an adaptive dead-time methodology so that both outputs (HO and LO) are never on at the same time, preventing cross conduction. Before the LO driver output is allowed to turn on, the adaptive dead-time logic first disables HO and waits for the HO voltage to drop below 1.5V typical. LO is allowed to turn on after a small delay (HO fall to LO rising delay). Similarly, the HO turn-on is delayed until the LO voltage has dropped below 1.5V. This technique makes sure of adequate dead-time for any size N-channel power MOSFET implementations, including parallel MOSFET configurations.

Caution is advised when adding series gate resistors, as this addition can impact the effective dead-time. The selected high-side MOSFET determines the appropriate bootstrap capacitance value  $C_{BOOT}$  in accordance with [Equation 13](#).

$$C_{BOOT} = \frac{Q_G}{\Delta V_{CBOOT}} \quad (13)$$

where

- $Q_G$  is the total gate charge of the high-side MOSFET at the applicable gate drive voltage.
- $\Delta V_{CBOOT}$  is the voltage variation of the high-side MOSFET driver after turn-on.

To determine  $C_{BOOT}$ , choose  $\Delta V_{CBOOT}$  such that the available gate drive voltage is not significantly impacted. An acceptable range of  $\Delta V_{CBOOT}$  is 100mV to 300mV. The bootstrap capacitor must be a low-ESR ceramic capacitor, typically 0.1 $\mu$ F. Select FETs to make sure that the minimum input supply voltage is higher than gate plateau voltage of the FET plus 0.5V so that the FET works in the ohmic region when turned on.

When the LM25190 is configured for a target output voltage smaller than 7.5V, the internal bootstrap UV circuit can source a 25 $\mu$ A current out of the SW pin. In the light load or no load case where the resistance of the feedback divider is not low enough to sink the extra amount of current, some dummy load is required to bleed off the charge on the output capacitors.

## 6.4 Device Functional Modes

### 6.4.1 Sleep Mode

The LM25190 operates with peak current-mode control such that the compensation voltage is proportional to the peak inductor current. During no-load or light-load conditions, the output capacitor discharges very slowly. As a result, the compensation voltage does not demand the driver output pulses on a cycle-by-cycle basis. When the LM25190 controller detects 16 missed switching cycles, the controller enters sleep mode and switches to a low  $I_Q$  state to reduce the current drawn from the input. For the LM25190 to go into sleep mode, the controller must be programmed for diode emulation (tie FPWM/SYNC to AGND).

The typical controller  $I_Q$  in sleep mode is 15 $\mu$ A with a 12V output.

### 6.4.2 Forced PWM Mode and Synchronization (FPWM/SYNC)

A synchronous buck regulator implemented with a low-side synchronous MOSFET rather than a diode has the capability to sink negative current from the output during conditions of, light-load, output overvoltage, and prebias start-up conditions. The LM25190 provides a diode emulation feature that can be enabled to prevent reverse (drain-to-source) current flow in the low-side MOSFET. When configured for diode emulation mode, the low-side MOSFET is switched off when reverse current flow is detected by sensing the SW voltage using a zero-cross comparator. The benefit of this configuration is lower power loss during light-load conditions. The disadvantage of diode emulation mode is slower light-load transient response.

The FPWM/SYNC pin configures diode emulation mode and forced PWM mode. To enable diode emulation and thus achieve low- $I_Q$  current at light loads, connect FPWM/SYNC to AGND. If FPWM with continuous conduction mode (CCM) operation is desired, tie FPWM/SYNC to VCC. Note that diode emulation is automatically engaged to prevent reverse current flow during a prebias start-up. A gradual change from DCM to CCM operation provides monotonic start-up performance.

To synchronize the LM25190 to an external source, apply a logic-level clock to the FPWM/SYNC pin. The LM25190 can be synchronized to  $\pm 20\%$  of the programmed frequency up to a maximum of 2.5MHz. When the LM25190 is operating in synchronization mode, LM25190 operates in FPWM mode. If there is an RT resistor tied to AGND and a synchronization signal, the LM25190 ignores the RT resistor and synchronizes to the external clock. If there is an RT resistor tied to VCC and a synchronization signal, the synchronization signal is ignored and the LM25190 operates in RT defined frequency with DRSS. Under low  $V_{IN}$  conditions when the minimum off time is reached, the synchronization signal is ignored, allowing the switching frequency to reduce to maintain output voltage regulation.

### 6.4.3 Thermal Shutdown

The LM25190 includes an internal junction temperature monitor. If the temperature exceeds 175°C (typical), thermal shutdown occurs. When entering thermal shutdown, the device:

1. Turns off the high-side and low-side MOSFETs.
2. PG/SYNCOUT switches low.
3. Turns off the VCC regulator.
4. Initiates a soft-start sequence when the die temperature decreases by the thermal shutdown hysteresis of 15°C (typical).

This protection is a non-latching protection, and, as such, the device cycles into and out of thermal shutdown if the fault persists.

## 7 Application and Implementation

### Note

Information in the following applications sections is not part of the TI component specification, and TI does not warrant its accuracy or completeness. TI's customers are responsible for determining suitability of components for their purposes, as well as validating and testing their design implementation to confirm system functionality.

### 7.1 Application Information

#### 7.1.1 Power Train Components

A comprehensive understanding of the buck regulator power train components is critical to successfully completing a synchronous buck regulator design. The following sections discuss the output inductor, input and output capacitors, power MOSFETs, and EMI input filter.

##### 7.1.1.1 Buck Inductor

For most applications, choose a buck inductance such that the inductor ripple current,  $\Delta I_L$ , is between 30% to 50% of the maximum DC output current at typical input voltage. Choose the inductance using [Equation 14](#).

$$L_0 = \frac{V_{OUT}}{\Delta I_L \times f_{SW}} \times \left(1 - \frac{V_{OUT}}{V_{IN}}\right) \quad (14)$$

Check the inductor data sheet to make sure that the saturation current of the inductor is above the peak inductor current of a particular design. Ferrite cores have very low core loss and are preferred at high switching frequencies, so design goals can then concentrate on copper loss and preventing saturation. Low inductor core loss is evidenced by reduced no-load input current and higher light-load efficiency. However, ferrite core materials exhibit a hard saturation characteristic and the inductance collapses abruptly when the saturation current is exceeded. This action results in an abrupt increase in inductor ripple current and higher output voltage ripple, not to mention reduced efficiency and compromised reliability. Note that the saturation current of an inductor generally decreases as the core temperature increases.

##### 7.1.1.2 Output Capacitors

The output capacitor combined with the control loop response make sure the output voltage stays within the dynamic transient tolerance specifications. The usual boundaries restricting the output capacitor are driven by finite available PCB area, component size, and cost. The equivalent series resistance (ESR) and equivalent series inductance (ESL) of the output capacitor dominates shaping the load transient response as the load step amplitude and slew rate increase.

The output capacitor,  $C_{OUT}$ , filters the inductor ripple current and provides a reservoir of charge for load transient events. Typically, ceramic capacitors provide low ESR to reduce the output voltage ripple and noise spikes, while tantalum or electrolytic capacitors provide a large bulk capacitance in a relatively compact footprint for transient loading events.

[Figure 7-1](#) conceptually illustrates the relevant current waveforms during both load step-down and step-up transitions. As shown, the large-signal slew rate of the inductor current is limited as the inductor current ramps to match the new load-current level following a load transient. This slew-rate limiting exacerbates the deficit of charge in the output capacitor, which must be replenished as fast as possible during and after the load step-up transient. Similarly, during and after a load step-down transient, the slew rate limiting of the inductor current adds to the surplus of charge in the output capacitor that must be depleted as quickly as possible.

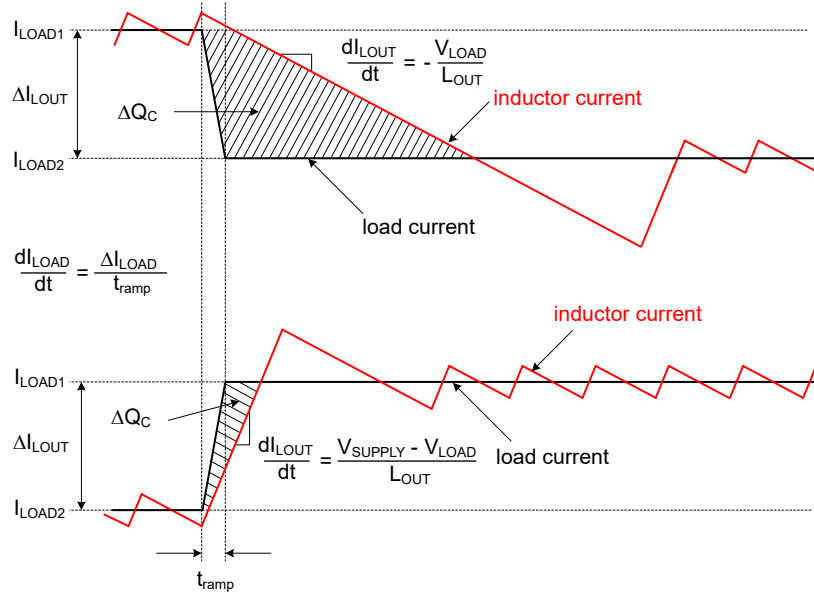


**Figure 7-1. Load Transient Response Representation Showing  $C_{OUT}$  Charge Surplus or Deficit**

For example, in a typical regulator application of 12V input to 3.3V output voltage, the load-off transient represents the worst case in terms of output voltage transient deviation. In that conversion ratio application, the steady-state duty cycle is approximately 28% and the large-signal inductor current slew rate when the duty cycle collapses to zero is approximately  $-V_{LOAD} / L_{OUT}$ . Compared to a load-on transient, the inductor current takes much longer to transition to the required level. The surplus of charge in the output capacitor causes the output voltage to overshoot. In fact, to deplete this excess charge from the output capacitor as quickly as possible, the inductor current must ramp below the nominal level following the load step. In this scenario, a large output capacitance can be advantageously employed to absorb the excess charge and minimize the voltage overshoot.

To meet the dynamic specification of output voltage overshoot during such a load-off transient (denoted as  $\Delta V_{OVERSHOOT}$  with step reduction in output current given by  $\Delta I_{LOAD}$ ), the output capacitance must be larger than:

$$C_{OUT} \geq \frac{L_{OUT} \times \Delta I_{LOAD}^2}{(V_{LOAD} + \Delta V_{OVERSHOOT})^2 - V_{LOAD}^2} \quad (15)$$

Based on the static specification of peak-to-peak output voltage ripple denoted by  $\Delta V_{LOAD}$ , choose an output capacitance that is larger than that given by [Equation 16](#).

$$C_{OUT} \geq \frac{\Delta I_{L_{OUT}}}{8 \times f_{SW} \times \sqrt{\Delta V_{LOAD}^2 - (R_{ESR} \times \Delta I_{L_{OUT}})^2}} \quad (16)$$

The ESR of a capacitor is provided in the manufacturer data sheet, either explicitly as a specification or implicitly in the impedance versus frequency curve. Depending on type, size, and construction, electrolytic capacitors have significant ESR, 5mΩ and above, and relatively large ESL, 5nH to 20nH. PCB traces contribute some parasitic resistance and inductance as well. Ceramic output capacitors have low-ESR and ESL contributions at the switching frequency, and the capacitive impedance component dominates. However, depending on package and voltage rating of the ceramic capacitor, the effective capacitance can drop quite significantly with applied DC voltage and operating temperature.

Ignoring the ESR term in [Equation 16](#) gives a quick estimation of the minimum ceramic capacitance necessary to meet the output ripple specification. Use [Equation 15](#) to determine if additional capacitance is necessary to meet the load-off transient overshoot specification.

A composite implementation of ceramic and electrolytic capacitors highlights the rationale for paralleling capacitors of dissimilar chemistries yet complementary performance. The frequency response of each capacitor is accretive in that each capacitor provides desirable performance over a certain portion of the frequency range. While the ceramic provides excellent mid- and high-frequency decoupling characteristics with the low ESR and ESL to minimize the switching frequency output ripple, the electrolytic device with the large bulk capacitance provides low-frequency energy storage to cope with load transient demands.

### 7.1.1.3 Input Capacitors

Input capacitors are necessary to limit the input ripple voltage to the buck power stage due to switching-frequency AC currents. TI recommends using X7S or X7R dielectric ceramic capacitors to provide low impedance and high RMS current rating over a wide temperature range. To minimize the parasitic inductance in the switching loop, position the input capacitors as close as possible to the drain of the high-side MOSFET and the source of the low-side MOSFET. The input capacitor RMS current for a single-channel buck regulator is given by [Equation 17](#).

$$I_{CIN,rms} = \sqrt{D \times \left( I_{LOAD}^2 \times (1 - D) + \frac{\Delta I_{LOAD}^2}{12} \right)} \quad (17)$$

The highest input capacitor RMS current occurs at  $D = 0.5$ , at which point, the RMS current rating of the input capacitors must be greater than half the output current.

Ideally, the DC component of input current is provided by the input voltage source and the AC component by the input filter capacitors. Neglecting inductor ripple current, the input capacitors source current of amplitude  $(I_{LOAD} - I_{SUPPLY})$  during the  $D$  interval and sinks  $I_{SUPPLY}$  during the  $1-D$  interval. Thus, the input capacitors conduct a square-wave current of peak-to-peak amplitude equal to the output current. The resultant capacitive component of AC ripple voltage is a triangular waveform. Together with the ESR-related ripple component, the peak-to-peak ripple voltage amplitude is given by [Equation 18](#).

$$\Delta V_{SUPPLY} = \frac{I_{LOAD} \times D \times (1 - D)}{f_{SW} \times C_{IN}} + I_{LOAD} \times R_{ESR} \quad (18)$$

The input capacitance required for a particular load current, based on an input voltage ripple specification of  $\Delta V_{SUPPLY}$ , is given by [Equation 19](#).

$$C_{IN} \geq \frac{D \times (1 - D) \times I_{LOAD}}{f_{SW} \times (\Delta V_{SUPPLY} - I_{LOAD} \times R_{ESR})} \quad (19)$$

Low-ESR ceramic capacitors can be placed in parallel with higher valued bulk capacitance to provide optimized input filtering for the regulator and damping to mitigate the effects of input parasitic inductance resonating with high-Q ceramics. Select the input bulk capacitor based on the ripple current rating and operating temperature range.

### 7.1.1.4 Power MOSFETs

The choice of power MOSFETs has significant impact on DC/DC regulator performance. A MOSFET with low on-state resistance,  $R_{DS(on)}$ , reduces conduction loss, whereas low parasitic capacitances enable faster transition times and reduced switching loss. Normally, the lower the  $R_{DS(on)}$  of a MOSFET, the higher the gate charge and output charge ( $Q_G$  and  $Q_{OSS}$ , respectively), and vice versa. As a result, the product of  $R_{DS(on)}$  and  $Q_G$  is commonly specified as a MOSFET figure-of-merit. Low thermal resistance of a given package makes sure that the MOSFET power dissipation does not result in excessive MOSFET die temperature.

The main parameters affecting power MOSFET selection are as follows:

- $R_{DS(on)}$  at 7.5V.
- Drain-source voltage rating,  $BV_{DSS}$ .
- Gate charge parameters at 7.5V.
- Output charge,  $Q_{OSS}$ , at the relevant input voltage.

- Body diode reverse recovery charge,  $Q_{RR}$ .
- Gate threshold voltage,  $V_{GS(th)}$ , derived from the Miller plateau evident in the  $Q_G$  versus  $V_{GS}$  plot in the MOSFET data sheet. To enhance MOSFET adequately, the miller plateau voltage must be 2V to 3V lower than the gate drive amplitude, especially at the minimum input voltage.

The MOSFET-related power losses for one channel are summarized by the equations presented in [Table 7-1](#), where suffixes one and two represent high-side and low-side MOSFET parameters, respectively. While the influence of inductor ripple current is considered, second-order loss modes, such as those related to parasitic inductances and SW node ringing, are not included.

**Table 7-1. MOSFET Power Losses**

POWER LOSS MODE	HIGH-SIDE MOSFET	LOW-SIDE MOSFET
MOSFET conduction (2) (3)	$P_{cond1} = D \times \left( I_{LOAD}^2 + \frac{\Delta I_{LOUT}^2}{12} \right) \times R_{DS(on)1}$ (20)	$P_{cond2} = D' \times \left( I_{LOAD}^2 + \frac{\Delta I_{LOUT}^2}{12} \right) \times R_{DS(on)2}$ (21)
MOSFET switching	$P_{sw1} = \frac{V_{SUPPLY} \times f_{SW}}{2} \times \left[ \left( I_{LOAD} - \frac{\Delta I_{LOUT}}{2} \right) \times t_R + \left( I_{LOAD} + \frac{\Delta I_{LOUT}}{2} \right) \times t_F \right]$ (22)	Negligible
MOSFET gate drive(1)	$P_{gate1} = V_{CC} \times f_{SW} \times Q_{G1}$ (23)	$P_{gate2} = V_{CC} \times f_{SW} \times Q_{G2}$ (24)
MOSFET output charge(4)	$P_{Coss} = f_{SW} \times (V_{SUPPLY} \times Q_{OSS2} + E_{oss1} - E_{oss2})$ (25)	
Body diode conduction	N/A	$P_{condBD} = V_F \times f_{SW} \times \left[ \left( I_{LOAD} + \frac{\Delta I_{LOUT}}{2} \right) \times t_{dt1} + \left( I_{LOAD} - \frac{\Delta I_{LOUT}}{2} \right) \times t_{dt2} \right]$ (26)
Body diode reverse recovery(5)	$P_{RR} = V_{SUPPLY} \times f_{SW} \times Q_{RR2}$ (27)	

- (1) Gate drive loss is apportioned based on the internal gate resistance of the MOSFET, externally added series gate resistance and the relevant driver resistance of the device.
- (2) MOSFET  $R_{DS(on)}$  has a positive temperature coefficient of approximately 4500ppm/°C. The MOSFET junction temperature,  $T_J$ , and the rise over ambient temperature is dependent upon the device total power dissipation and the thermal impedance. When operating at or near minimum input voltage, make sure that the MOSFET  $R_{DS(on)}$  is rated for the available gate drive voltage.
- (3)  $D' = 1-D$  is the duty cycle complement.
- (4) MOSFET output capacitances,  $C_{oss1}$  and  $C_{oss2}$ , are highly non-linear with voltage. These capacitances are charged losslessly by the inductor current at high-side MOSFET turn-off. During turn-on, however, a current flows from the input to charge the output capacitance of the low-side MOSFET.  $E_{oss1}$ , the energy of  $C_{oss1}$ , is dissipated at turn-on, but this dissipation is offset by the stored energy  $E_{oss2}$  on  $C_{oss2}$ .
- (5) MOSFET body diode reverse recovery charge,  $Q_{RR}$ , depends on many parameters, particularly forward current, current transition speed, and temperature.

The high-side (control) MOSFET carries the inductor current during the PWM on-time (or D interval) and typically incurs most of the switching losses. Choosing a high-side MOSFET that balances conduction and switching loss contributions is imperative. The total power dissipation in the high-side MOSFET is the sum of the losses due to conduction, switching (voltage-current overlap), output charge, and typically two-thirds of the net loss attributed to body diode reverse recovery.

The low-side (synchronous) MOSFET carries the inductor current when the high-side MOSFET is off (or 1–D interval). The low-side MOSFET switching loss is negligible as the low-side MOSFET switching loss is switched at zero voltage – current just commutates from the channel to the body diode or vice versa during the

transition dead-times. The device, with the adaptive gate drive timing, minimizes body diode conduction losses when both MOSFETs are off. Such losses scale directly with switching frequency.

In high step-down ratio applications, the low-side MOSFET carries the current for a large portion of the switching period. Therefore, to attain high efficiency, optimizing the low-side MOSFET for low  $R_{DS(on)}$  is critical. In cases where the conduction loss is too high or the target  $R_{DS(on)}$  is lower than available in a single MOSFET, connect two low-side MOSFETs in parallel. The total power dissipation of the low-side MOSFET is the sum of the losses due to channel conduction, body diode conduction, and typically one-third of the net loss attributed to body diode reverse recovery.

### 7.1.1.5 EMI Filter

Switching regulators exhibit negative input impedance, which is lowest at the minimum input voltage. An underdamped LC filter exhibits a high output impedance at the resonant frequency of the filter. For stability, the filter output impedance must be less than the absolute value of the converter input impedance.

$$Z_{IN} = \left| -\frac{V_{SUPPLY(MIN)}^2}{P_{SUPPLY}} \right| \quad (28)$$

The passive EMI filter design steps are as follows:

- Calculate the required attenuation of the EMI filter at the switching frequency, where  $C_{IN}$  represents the existing capacitance at the input of the switching converter.
- Input filter inductor  $L_F$  is usually selected between  $1\mu\text{H}$  and  $10\mu\text{H}$ , but can be lower to reduce losses in a high-current design.
- Calculate input filter capacitor  $C_F$ .

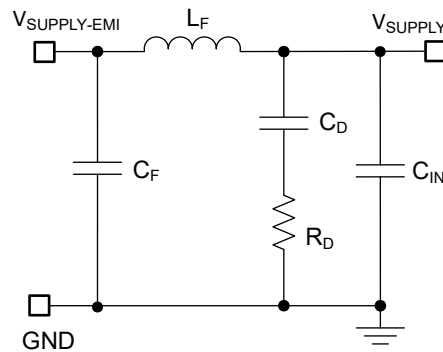


**Figure 7-2. Passive  $\pi$ -Stage EMI Filter for Buck Regulator**

By calculating the first harmonic current from the Fourier series of the input current waveform and multiplying by the input impedance (the impedance is defined by the existing input capacitor  $C_{IN}$ ), a formula is derived to obtain the required attenuation as shown by [Equation 29](#).

$$\text{Attn} = 20\log\left(\frac{I_{L\text{OUT(PEAK)}}}{\pi^2 \times f_{SW} \times C_{IN}} \times \sin(\pi \times D_{MAX}) \times \frac{1}{11V}\right) - V_{MAX} \quad (29)$$

where

- $V_{MAX}$  is the allowed dB $\mu\text{V}$  noise level for the applicable conducted EMI specification.
- $C_{IN}$  is the existing input capacitance of the buck regulator.
- $D_{MAX}$  is the maximum duty cycle.
- $I_{L\text{OUT(PEAK)}}$  is the peak inductor current.

For filter design purposes, the current at the input can be modeled as a square-wave. Determine the passive EMI filter capacitance  $C_F$  from [Equation 30](#).

$$C_F = \frac{1}{L_F} \left( \frac{|Attn|}{2\pi \times f_{SW}} \right)^2 \quad (30)$$

Adding an input filter to a switching regulator modifies the control-to-output transfer function. The output impedance of the filter must be sufficiently small so that the input filter does not significantly affect the loop gain of the buck converter. The impedance peaks at the filter resonant frequency. The resonant frequency of the passive filter is given by [Equation 31](#).

$$f_{res} = \frac{1}{2\pi \times \sqrt{L_F \times C_F}} \quad (31)$$

The purpose of  $R_D$  is to reduce the peak output impedance of the filter at the resonant frequency. Capacitor  $C_D$  blocks the DC component of the input voltage to avoid excessive power dissipation in  $R_D$ . Capacitor  $C_D$  must have lower impedance than  $R_D$  at the resonant frequency with a capacitance value greater than that of the input capacitor  $C_{IN}$ . This requirement prevents  $C_{IN}$  from interfering with the cutoff frequency of the main filter. Added input damping is needed when the output impedance of the filter is high at the resonant frequency ( $Q$  of filter formed by  $L_F$  and  $C_{IN}$  is too high). An electrolytic capacitor  $C_D$  can be used for input damping with a value given by [Equation 32](#).

$$C_D \geq 4 \times C_{IN} \quad (32)$$

Select the input damping resistor  $R_D$  using [Equation 33](#).

$$R_D = \sqrt{\frac{L_F}{C_{IN}}} \quad (33)$$

### 7.1.2 Error Amplifier and Compensation

[Figure 7-3](#) shows a type-II compensator using a transconductance error amplifier (EA). The dominant pole of the EA open-loop gain is set by the EA output resistance,  $R_{O(EA)}$ , and effective bandwidth-limiting capacitance,  $C_{BW}$ , as shown by [Equation 34](#).

$$G_{EA}(s) = - \frac{g_{m(EA)} \times R_{O(EA)}}{1 + s \times R_{O(EA)} \times C_{BW}} \quad (34)$$

The EA high-frequency pole is neglected in the above expression. [Equation 35](#) calculates the compensator transfer function from output voltage to COMP node, including the gain contribution from the (internal or external) feedback resistor network.

$$G_{COMP}(s) = \frac{V_{COMP}(s)}{V_{LOAD}(s)} = - \frac{V_{REF}}{V_{LOAD}} \times \frac{g_m \times R_{O(EA)} \times \left(1 + \frac{s}{\omega_{Z1}}\right)}{\left(1 + \frac{s}{\omega_{P1}}\right) \times \left(1 + \frac{s}{\omega_{P2}}\right)} \quad (35)$$

where

- $V_{REF}$  is the feedback voltage reference.
- $g_{m(EA)}$  is the EA gain transconductance of 1mS.
- $R_{O(EA)}$  is the error amplifier output impedance of 70M $\Omega$ .

$$\omega_{Z1} = \frac{1}{R_{COMP} \times C_{COMP}} \quad (36)$$

$$\omega_{P1} = \frac{1}{R_{O(EA)} \times (C_{COMP} + C_{HF} + C_{BW})} \cong \frac{1}{R_{O(EA)} \times C_{COMP}} \quad (37)$$

$$\omega_{P2} = \frac{1}{R_{COMP} \times (C_{COMP} || (C_{HF} + C_{BW}))} \cong \frac{1}{R_{COMP} \times C_{HF}} \quad (38)$$

The EA compensation components create a pole close to the origin, a zero, and a high-frequency pole. Typically,  $R_{COMP} \ll R_{O(EA)}$  and  $C_{COMP} \gg C_{BW}$  and  $C_{HF}$ , so the approximations are valid.

LM25190 uses FB as the feedback pin for the sensed output voltage. If there is a ground offset between local ground and remote output ground, there is a regulation error due to the sensing error. In this case, AGND pin can be used with FB pin to provide a more accurate regulation. LM25190 allows AGND to deviate as much as +/-300mV typical with respect to PGND.

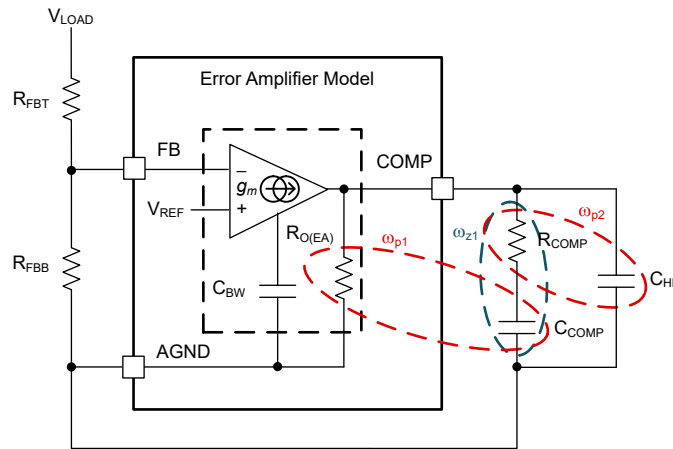


Figure 7-3. Error Amplifier and Compensation Network

## 7.2 Typical Applications

### 7.2.1 High Efficiency 2.1MHz CC-CV Regulator

Figure 7-4 shows the typical schematic diagram of a CC-CV buck regulator. In this example, the CV regulation target is 5V and the CC regulation target is 5A. Full-load efficiency is 91.6% at 12V input. The switching frequency is set at 2.1MHz by resistor  $R_{RT}$ .

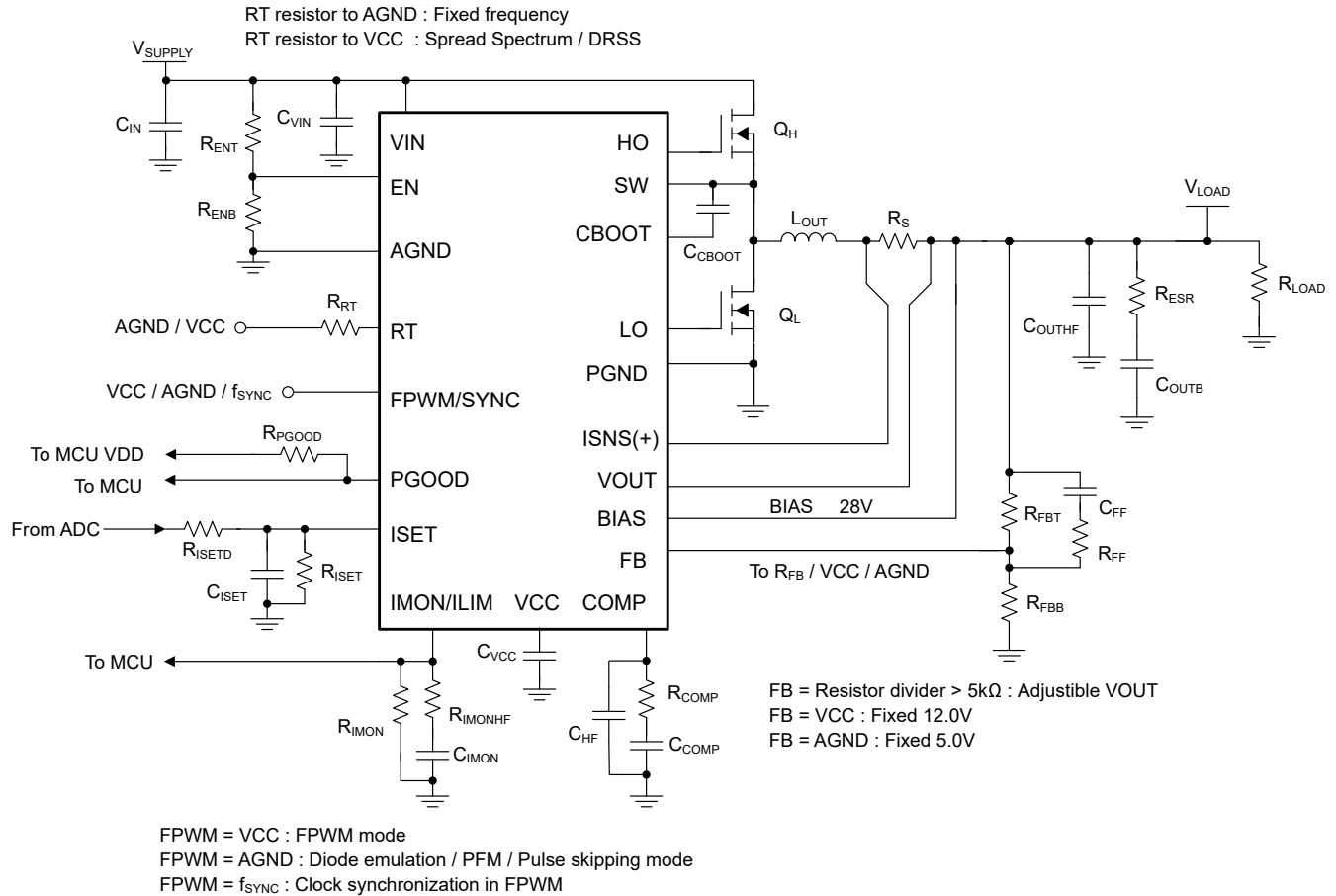


Figure 7-4. Typical CC-CV Buck Regulator Circuit

#### Note

Depending on the source impedance of the input supply bus, an electrolytic capacitor can be required at the input to make sure of stability, particularly at low input voltage and high output current operating conditions. See Section 7.3 for more details.

### 7.2.1.1 Design Requirements

The following table shows the intended input, output, and performance parameters for this design example.

**Table 7-2. Design Parameters**

DESIGN PARAMETER	VALUE
Input operating range	5.5V, 12V, 42V (minimum, typical, maximum)
CV regulation target	5V
CC regulation target	5A
Switching frequency	2100kHz

The switching frequency is set at 2100KHz by resistor  $R_{RT}$ . In terms of control loop performance, the target loop crossover frequency is 60kHz with a phase margin greater than 60°.

### 7.2.1.2 Detailed Design Procedure

Use the Quick Start Calculator to expedite the process of designing a regulator for a given application based on the device specifications. Download the [LM25190-LM5190-DESIGN-CALC](#) Quick Start Calculator for a detailed design procedure.

See the [LM25190-Q1 CCCV Buck Controller Evaluation Module](#) EVM user's guide for recommended components and typical application curves.

#### 7.2.1.2.1 Buck Inductor

1. Use the following equation to calculate the required buck inductance based on a 40% inductor ripple current at nominal input voltages.

$$L_O = \frac{V_{OUT}}{\Delta I_L \times f_{SW}} \times \left(1 - \frac{V_{OUT}}{V_{IN}}\right) = \frac{5}{2 \times 2100k} \times \left(1 - \frac{5}{12}\right) = 0.69\mu\text{H} \quad (39)$$

2. Select a standard inductor value of 0.68μH to account for effective inductance derating with current of molded inductors. Use the following equation to calculate the peak inductor currents at maximum steady-state input voltage.

$$I_{LO(PK)} = I_{LOAD} + \frac{\Delta I_L}{2} = I_{LOAD} + \frac{V_{OUT}}{2 \times L_O \times f_{SW}} \times \left(1 - \frac{V_{OUT}}{V_{IN(MAX)}}\right) = 5 + \frac{3.085}{2} = 6.54\text{A} \quad (40)$$

3. Subharmonic oscillation occurs with a duty cycle greater than 50% for peak current-mode control. For design simplification, the device has an internal slope compensation ramp proportional to the switching frequency that is added to the current sense signal to damp any tendency toward subharmonic oscillation. Use the following equation to cross-check the inductance to set a slope compensation close to the ideal one times the inductor current downslope.

$$L_{O(MIN)} = \frac{V_{OUT} \times R_S}{0.08 \times f_{SW}} = \frac{5 \times 7m}{0.08 \times 2100k} = 0.21\mu\text{H} \quad (41)$$

#### 7.2.1.2.2 Current-Sense Resistance

1. Calculate the current-sense resistance based on a maximum peak current capability of at least 20% higher than the peak inductor current at full load to provide sufficient margin during start-up and load-on transients. Calculate the current sense resistances using the following equation.

$$R_S = \frac{V_{CS-TH}}{1.2 \times I_{LO(PK)}} = \frac{60m}{1.2 \times 6.54} = 7.6\text{m}\Omega \quad (42)$$

2. Select a standard resistance value of 7mΩ for the shunt. Carefully adhere to the layout guidelines in [Section 7.4.1](#) to make sure that noise and DC errors do not corrupt the differential current-sense voltages measured at the ISNS+ and VOUT pins.
3. Place the shunt resistor close to the inductor.
4. Use Kelvin-sense connections, and route the sense lines differentially from the shunt to the device.

- The CS-to-output propagation delay (related to the current limit comparator, internal logic, and power MOSFET gate drivers) causes the peak current to increase above the calculated current limit threshold. For a total propagation delay  $t_{\text{DELAY}}$  of 75ns, use the following equation to calculate the worst-case peak inductor current with the output shorted.

$$I_{\text{LO-PK(SC)}} = \frac{V_{\text{CS-TH(MAX)}}}{R_{\text{S}}} + \frac{V_{\text{IN(MAX)}} \times t_{\text{DELAY}}}{L_{\text{O}}} = \frac{68\text{m}}{7\text{m}} + \frac{42 \times 75\text{n}}{0.68\mu} = 14.3\text{A} \quad (43)$$

- Based on this result, select an inductor with saturation current greater than 14.3A across the full operating temperature range.

#### 7.2.1.2.3 Output Capacitors

- Use the following equation to estimate the output capacitance required to manage the output voltage overshoot during a load-off transient (from full load to no load) assuming a load transient deviation specification of 1% .

$$C_{\text{OUT}} \geq \frac{L_{\text{O}} \times \Delta I_{\text{LOAD}}^2}{(V_{\text{LOAD}} + \Delta V_{\text{OVERSHOOT}})^2 - V_{\text{LOAD}}^2} = \frac{0.68\mu \times 5^2}{(5 + 5 \times 0.01)^2 - 5^2} = 34\mu\text{F} \quad (44)$$

- Noting the voltage coefficient of ceramic capacitors where the effective capacitance decreases significantly with applied voltage, select four 47 $\mu\text{F}$ , 10V, 1210 ceramic output capacitors. Generally, when sufficient capacitance is used to satisfy the load-off transient response requirement, the voltage undershoot during a no-load to full-load transient is also satisfactory.
- Use the following equation to estimate the peak-peak output voltage ripple at nominal input voltage.

$$\Delta V_{\text{OUT}} = \sqrt{\left(\frac{\Delta I_{\text{L}}}{8 \times f_{\text{SW}} \times C_{\text{OUT}}}\right)^2 + (R_{\text{ESR}} \times \Delta I_{\text{L}})^2} = \sqrt{\left(\frac{3.085}{8 \times 2100\text{k} \times 94\mu}\right)^2 + (2\text{m} \times 3.085)^2} = 6.5\text{mV} \quad (45)$$

where

- $R_{\text{ESR}}$  is the effective equivalent series resistance (ESR) of the output capacitors.
  - 94 $\mu\text{F}$  is the total effective (derated) ceramic output capacitance at 5V.
- Use the following equation to calculate the output capacitor RMS ripple current and verify that the ripple current is within the capacitor ripple current rating.

$$I_{\text{CO(RMS)}} = \frac{\Delta I_{\text{L(OUT)}}}{\sqrt{12}} = \frac{3.085}{\sqrt{12}} = 0.89\text{A} \quad (46)$$

#### 7.2.1.2.4 Input Capacitors

A power supply input typically has a relatively high source impedance at the switching frequency. Good-quality input capacitors are necessary to limit the input ripple voltage. As mentioned earlier, dual-channel interleaved operation significantly reduces the input ripple amplitude. In general, the ripple current splits between the input capacitors based on the relative impedance of the capacitors at the switching frequency.

- Select the input capacitors with sufficient voltage and RMS ripple current ratings.
- Use the following equation to calculate the input capacitor RMS ripple current assuming a worst-case duty-cycle operating point of 50%.

$$I_{\text{CIN,rms}} = \sqrt{D \times \left( I_{\text{LOAD}}^2 \times (1 - D) + \frac{\Delta I_{\text{L(OUT)}}^2}{12} \right)} = \sqrt{0.5 \times \left( 5^2 \times (1 - 0.5) + \frac{3.085^2}{12} \right)} = 2.6\text{A} \quad (47)$$

- Use the following equation to find the required input capacitance.

$$C_{\text{IN}} \geq \frac{D \times (1 - D) \times I_{\text{LOAD}}}{f_{\text{SW}} \times (\Delta V_{\text{SUPPLY}} - I_{\text{LOAD}} \times R_{\text{ESR}})} = \frac{0.5 \times (1 - 0.5) \times 5}{2100\text{k} \times (0.25 - 5 \times 1\text{m})} = 2.4\mu\text{F} \quad (48)$$

where

- $\Delta V_{\text{SUPPLY}}$  is the input peak-to-peak ripple voltage specification.
- $R_{\text{ESR}}$  is the input capacitor ESR.

4. Recognizing the voltage coefficient of ceramic capacitors, select six 4.7μF, 100V, X7R, 1210 ceramic input capacitors. Place these capacitors adjacent to the power MOSFETs. See [Section 7.4.1.1](#) for more details.
5. Use six 10nF, 100V, X7R, 0603 ceramic capacitors near the high-side MOSFET to supply the high di/dt current during MOSFET switching transitions. Such capacitors offer high self-resonant frequency (SRF) and low effective impedance above 100MHz. The result is lower power loop parasitic inductance, thus minimizing switch-node voltage overshoot and ringing for lower conducted and radiated EMI signature. Refer to [Section 7.4.1](#) for more details.

#### 7.2.1.2.5 Frequency Set Resistor

Calculate the RT resistance for a switching frequency of 2100kHz using the following equation.

$$R_{RT} = \frac{\frac{10^{12}}{f_{SW}} - 59k}{41} = \frac{\frac{10^{12}}{2100k} - 59k}{41} = 10.2k\Omega \quad (49)$$

#### 7.2.1.2.6 Feedback Resistors

If an output voltage setpoint other than 5.0V or 12V is required (or to measure a bode plot when using either of the fixed output voltage options), determine the feedback resistances using the following equation.

$$R_{FBT} = R_{FBB} \times \left( \frac{V_{OUT}}{V_{REF}} - 1 \right) = 19.05k \times \left( \frac{5}{0.8} - 1 \right) = 100k\Omega \quad (50)$$

7.2.1.3 Application Curves

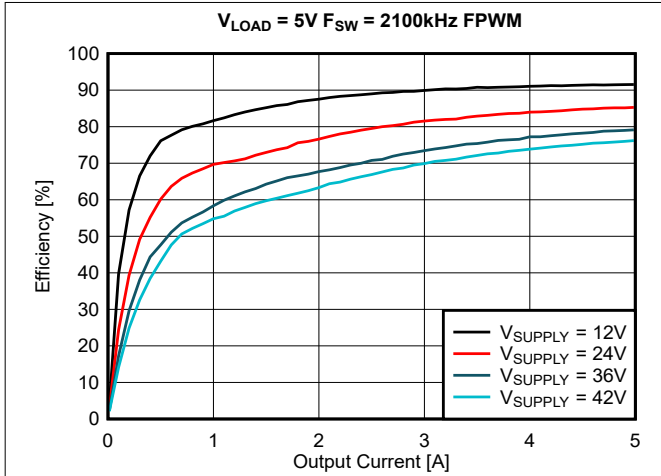


Figure 7-5. FPWM Mode Efficiency, Linear Scale

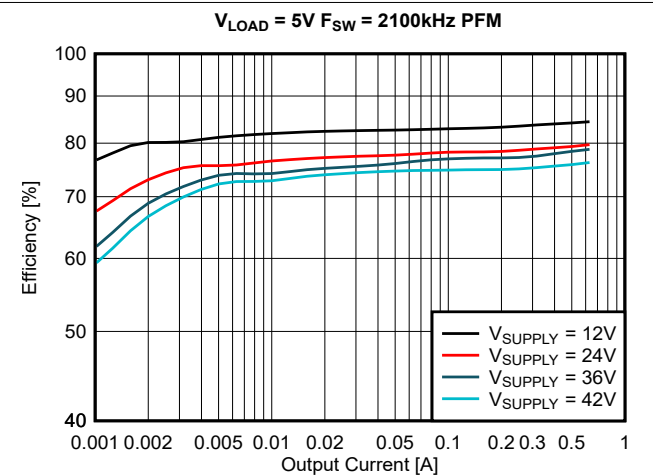


Figure 7-6. PFM Mode Efficiency, Log Scale

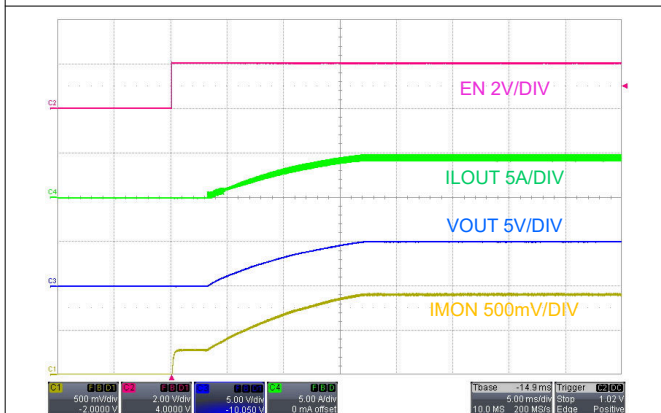


Figure 7-7. Start-Up, EN ON,  $V_{SUPPLY} = 12V$ ,  $I_{LOAD} = 5A$  Resistive Load

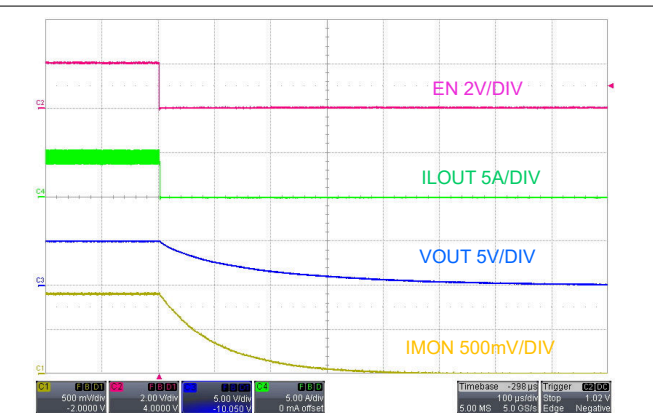


Figure 7-8. Shutdown, EN OFF,  $V_{SUPPLY} = 12V$ ,  $I_{LOAD} = 5A$  Resistive Load

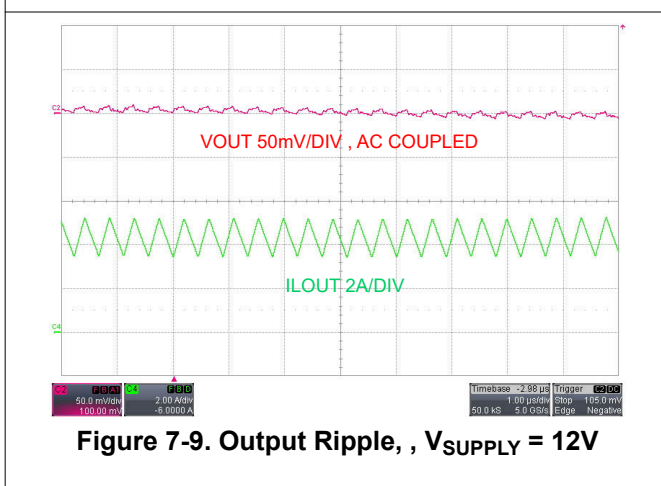


Figure 7-9. Output Ripple,  $V_{SUPPLY} = 12V$

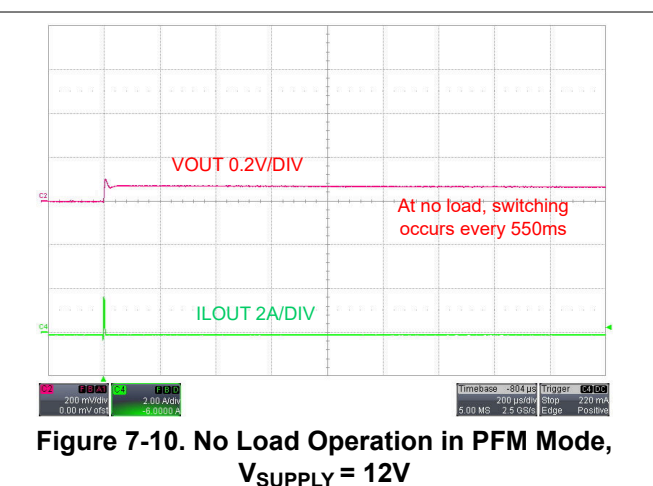
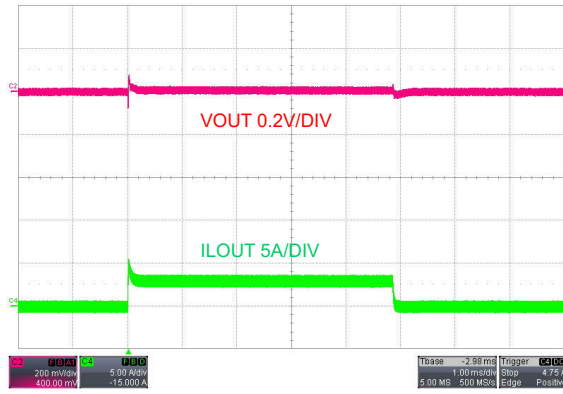
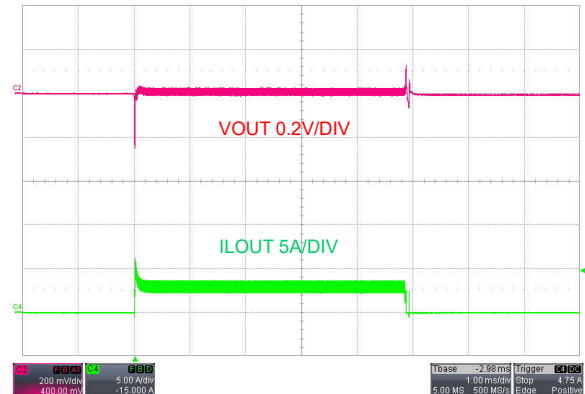


Figure 7-10. No Load Operation in PFM Mode,  $V_{SUPPLY} = 12V$



**Figure 7-11. Load Transient Response,  $V_{\text{SUPPLY}} = 12\text{V}$ , FPWM, 0A to 3A**



**Figure 7-12. Load Transient Response,  $V_{\text{SUPPLY}} = 12\text{V}$ , PFM, 0A to 3A**

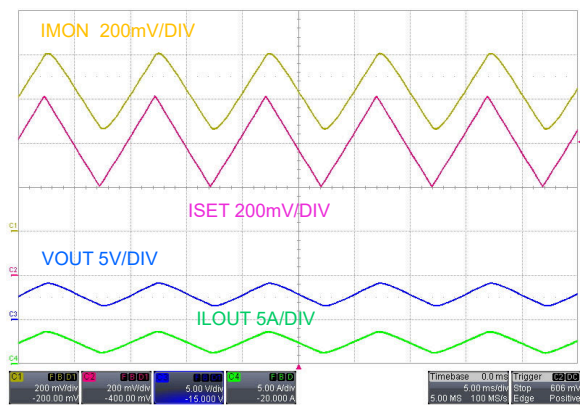


**Figure 7-13. ISET Modulation,  $V_{\text{SUPPLY}} = 12\text{V}$ ,  $R_{\text{LOAD}} = 1.0\Omega$**

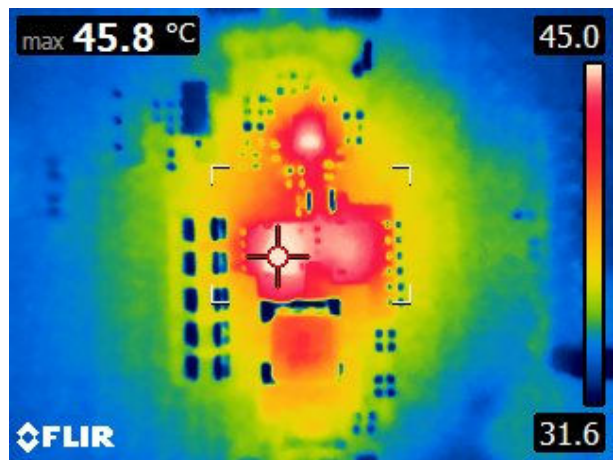


**Figure 7-14.  $V_{\text{SUPPLY}} = 12\text{V}$ ,  $I_{\text{LOAD}} = 5\text{A}$ ,  $T_{\text{A}} = 25^{\circ}\text{C}$ , No Airflow**

### 7.3 Power Supply Recommendations

The device is designed to operate from a wide input supply voltage range. The characteristics of the input supply must be compatible with the *Absolute Maximum Ratings* and *Recommended Operating Conditions*. In addition, the input supply must be capable of delivering the required input supply current to the fully loaded regulator. Estimate the average input supply current with [Equation 51](#).

$$I_{\text{SUPPLY}} = \frac{V_{\text{LOAD}} \times I_{\text{LOAD}}}{V_{\text{SUPPLY}} \times \text{Efficiency}} \quad (51)$$

If the regulator is connected to an input supply through long wires or PCB traces with a large impedance, take special care to achieve stable performance. The parasitic inductance and resistance of the input cables can have an adverse affect on converter operation. The parasitic inductance in combination with the low-ESR ceramic input capacitors form an underdamped resonant circuit. This circuit can cause overvoltage transients at the regulator input each time the input supply is cycled ON and OFF. The parasitic resistance causes the input supply voltage to dip during a load transient. The best way to solve such issues is to reduce the distance from the input supply to the regulator and use an aluminum or tantalum input capacitor in parallel with the ceramics. The moderate ESR of the electrolytic capacitors helps damp the input resonant circuit and reduce any voltage overshoots.

An EMI input filter is often used in front of the regulator that, unless carefully designed, can lead to instability as well as some of the effects mentioned above. The *AN-2162 Simple Success With Conducted EMI From DCDC Converters* application report provides helpful suggestions when designing an input filter for any switching regulator.

### 7.4 Layout

#### 7.4.1 Layout Guidelines

Proper PCB design and layout is important in a high-current, fast-switching circuit to achieve a robust and reliable design. The high power switching loop of a buck regulator power stage is denoted by loop 1 in the shaded area of [Figure 7-15](#). The topological architecture of a buck regulator means that particularly high di/dt current flows in the components of loop 1, reducing the parasitic inductance of this loop by minimizing the effective loop area becomes mandatory. Also important are the gate drive loops of the high-side and low-side MOSFETs, denoted by 3 and 4, respectively.

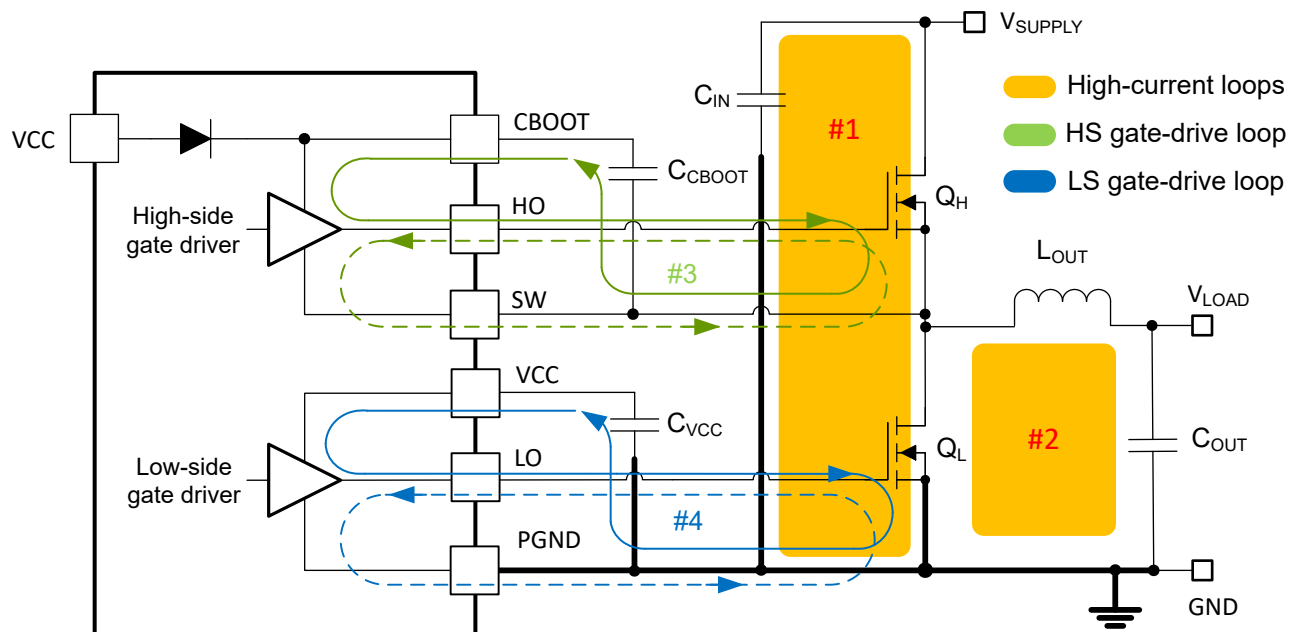


Figure 7-15. DC/DC Regulator Ground System With Power Stage and Gate Drive Circuit Switching Loops

#### 7.4.1.1 Power Stage Layout

- Input capacitors, output capacitors, and MOSFETs are the constituent components of the power stage of a buck regulator and are typically placed on the top side of the PCB. The benefits of convective heat transfer are maximized because of leveraging any system-level airflow. In a two-sided PCB layout, small-signal components are typically placed on the bottom side. Insert at least one inner plane, connected to ground, to shield and isolate the small-signal traces from noisy power traces and lines.
- The DC/DC regulator has several high-current loops. Minimize the area of these loops to suppress generated switching noise and optimize switching performance.
  - Loop 1: The most important loop area to minimize. The path is from the input capacitor or capacitors through the high- and low-side MOSFETs, and back to the capacitor or capacitors through the ground connection. Connect the input capacitor or capacitors negative terminal close to the source of the low-side MOSFET. Similarly, connect the input capacitor or capacitors positive terminal close to the drain of the high-side MOSFET.
  - Loop 2 : Loop 2 is not as critical as loop 1. The path is from the low-side MOSFET through the inductor and output capacitor or capacitors, and back to source of the low-side MOSFET through ground. Connect the source of the low-side MOSFET and negative terminal of the output capacitor or capacitors at ground as close as possible.
- The PCB trace defined as SW node, which connects to the source of the high-side MOSFET, the drain of the low-side MOSFET and the high-voltage side of the inductor, must be short and wide. However, the SW connection is a source of injected EMI and thus must not be too large.
- Follow any layout considerations of the MOSFETs as recommended by the MOSFET manufacturer, including pad geometry and solder paste stencil design.
- The SW pin connects to the switch node of the power conversion stage and acts as the return path for the high-side gate driver. The parasitic inductance inherent to loop 1 and the output capacitance ( $C_{OSS}$ ) of both power MOSFETs form a resonant circuit that induces high frequency ( $> 50\text{MHz}$ ) ringing at the SW node. The voltage peak of this ringing, if not controlled, can be significantly higher than the input voltage. Make sure that the peak ringing amplitude does not exceed the absolute maximum rating limit for the SW pin. In many cases, a series resistor and capacitor snubber network connected from the SW node to GND damps the ringing and decreases the peak amplitude. If testing reveals that the ringing amplitude at the SW pin is excessive, then include snubber components as needed.

#### 7.4.1.2 Gate-Drive Layout

Minimizing stray or parasitic gate loop inductance is key to optimizing gate drive switching performance, whether series gate inductance resonates with MOSFET gate capacitance or common source inductance (common to gate and power loops) provides a negative feedback component opposing the gate drive command, thereby increasing MOSFET switching times. The following loops are important:

- Loop 3: high-side MOSFET,  $Q_H$ . During the high-side MOSFET turn-on, high current flows from the bootstrap capacitor through the gate driver and high-side MOSFET, and back to the negative terminal of the boot capacitor through the SW connection. Conversely, to turn off the high-side MOSFET, high current flows from the gate of the high-side MOSFET through the gate driver and SW, and back to the source of the high-side MOSFET through the SW trace.
- Loop 4: low-side MOSFET,  $Q_L$ . During the low-side MOSFET turn-on, high current flows from the VCC decoupling capacitor through the gate driver and low-side MOSFET, and back to the negative terminal of the capacitor through ground. Conversely, to turn off the low-side MOSFET, high current flows from the gate of the low-side MOSFET through the gate driver and GND, and back to the source of the low-side MOSFET through ground.

TI recommends following circuit layout guidelines when designing with high-speed MOSFET gate drive circuits.

- Connections from gate driver outputs, HO and LO, to the respective gates of the high-side or low-side MOSFETs must be as short as possible to reduce series parasitic inductance. Be aware that peak gate drive currents can be as high as a few amperes. Use 0.65mm (25mils) or wider traces. Use via or vias, if necessary, of at least 0.6mm (20 mils) diameter along these traces. Route HO and SW traces as a differential pair from the device to the high-side MOSFET, taking advantage of flux cancellation. Also, route LO trace and

PGND trace/copper area as a differential pair from the device to the low-side MOSFET, taking advantage of flux cancellation.

- Locate the bootstrap capacitor,  $C_{CBOOT}$ , close to the CBOOT and SW pins of the device to minimize the area of loop 3 associated with the high-side driver. Similarly, locate the VCC capacitor,  $C_{VCC}$ , close to the VCC and PGND pins of the device to minimize the area of loop 4 associated with the low-side driver.

#### 7.4.1.3 PWM Controller Layout

Locate the device as close as possible to the power MOSFETs to minimize gate driver trace runs, the components related to the analog and feedback signals as well as current sensing are considered in the following:

- Separate power and signal/analog traces, and use a ground plane to provide noise shielding.
- Place all sensitive analog traces and components related to COMP, FB, ISNS+, IMON, ISET, and RT away from high-voltage switching nodes such as SW, HO, LO, or CBOOT to avoid mutual coupling. Use internal layer or layers as ground plane or planes. Pay particular attention to shielding the feedback (FB) and current sense (ISNS+ and VOUT) traces from power traces and components.
- Locate the upper and lower feedback resistors close to the FB pin, keeping the FB trace as short as possible. Route the trace from the upper feedback resistor to the required output voltage sense point at the load.
- Route the ISNS+ and VOUT sense traces as differential pairs to minimize noise pickup and use Kelvin connections to the applicable shunt resistor.
- Minimize the loop area from the VCC and VIN pins through the respective decoupling capacitors to the PGND pin. Locate these capacitors as close as possible to the device.

#### 7.4.1.4 Thermal Design and Layout

The operating temperature range of a PWM controller with integrated gate drivers and bias supply LDO regulator is greatly affected by the following:

- Average gate drive current requirements of the power MOSFETs
- Switching frequency
- Operating input supply voltage (affecting bias regulator LDO voltage drop and hence the power dissipation)
- Thermal characteristics of the package and operating environment

For a PWM controller to be useful over a particular temperature range, the package must allow for the efficient removal of the heat produced while keeping the junction temperature within rated limits.

The VQFN package offers a means of removing heat from the semiconductor die through the exposed thermal pad at the base of the package. The exposed pad of the package is thermally connected to the substrate of the device. This connection allows a significant improvement in heat sinking and becomes imperative that the PCB is designed with thermal lands, thermal vias, and a ground plane to complete the heat removal subsystem. The exposed pad of the device is soldered to the ground-connected copper land on the PCB directly underneath the device package, reducing the thermal resistance to a very low value.

Numerous vias with a 0.3mm diameter connected from the thermal land to the internal and solder-side ground plane or planes are vital to help dissipation. In a multi-layer PCB design, a solid ground plane is typically placed on the PCB layer below the power components. Not only does this placement provide a plane for the power stage currents to flow but this placement also represents a thermally conductive path away from the heat generating devices.

The thermal characteristics of the MOSFETs also are significant. The drain pads of the high-side MOSFETs are normally connected to a VIN plane for heat sinking. The drain pads of the low-side MOSFETs are tied to the SW plane, but the SW plane area is purposely kept as small as possible to mitigate EMI concerns.

#### 7.4.1.5 Ground Plane Design

TI recommends using one or more of the inner PCB layers as a solid ground plane. A ground plane offers shielding for sensitive circuits and traces and also provides a quiet reference potential for the control circuitry. In particular, a full ground plane on the layer directly underneath the power stage components is essential. Connect the source terminal of the low-side MOSFET and return terminals of the input and output capacitors to

this ground plane. Connect the PGND and AGND pins of the device at the exposed pad and then connect to the system ground plane using an array of vias under the exposed pad. The PGND nets contain noise at the switching frequency and can bounce because of load current variations. The power traces for PGND, VIN, and SW can be restricted to one side of the ground plane, for example on the top layer. The other side of the ground plane contains much less noise and is designed for sensitive analog trace routes.

#### 7.4.2 Layout Example

Figure 7-16 shows a layout example of a synchronous buck regulator with discrete power MOSFETs. The design uses an inner layer as a power-loop return path directly underneath the top layer to create a low-area switching power loop. This loop area, and hence parasitic inductance, must be as small as possible to minimize EMI as well as switch-node voltage overshoot and ringing.

The high-frequency power loop current flows through MOSFETs, through the power ground plane on the inner layer, and back to VIN through the 0603/1210 ceramic capacitors .

Six 0603 case size capacitors are placed in parallel very close to the drain of the high-side MOSFET. The low equivalent series inductance (ESL) and high self-resonant frequency (SRF) of the small footprint capacitors yield excellent high-frequency performance. The negative terminals of these capacitors are connected to the inner layer ground plane with multiple vias, further minimizing parasitic loop inductance.

Additional guidelines to improve noise immunity and reduce EMI are as follows:

- Connect PGND directly to the low-side MOSFET and power ground. Connect AGND directly to an analog ground plane for sensitive analog components. The analog ground plane for AGND and the power ground plane for PGND must be connected at a single point directly under the device at the exposed pad.
- Connect the MOSFETs directly to the inductor terminal with short copper connections (without vias) as this net has high  $dv/dt$  and contributes to radiated EMI. The single-layer routing of the switch-node connection means that switch-node vias with high  $dv/dt$  do not appear on the bottom side of the PCB. This avoids e-field coupling to the reference ground plane during the EMI test. VIN and PGND plane copper pours shield the polygon connecting the MOSFETs to the inductor terminal, further reducing the radiated EMI signature.
- Place the *EMI filter* components on the bottom side of the PCB so that the components are shielded from the power stage components on the top side.

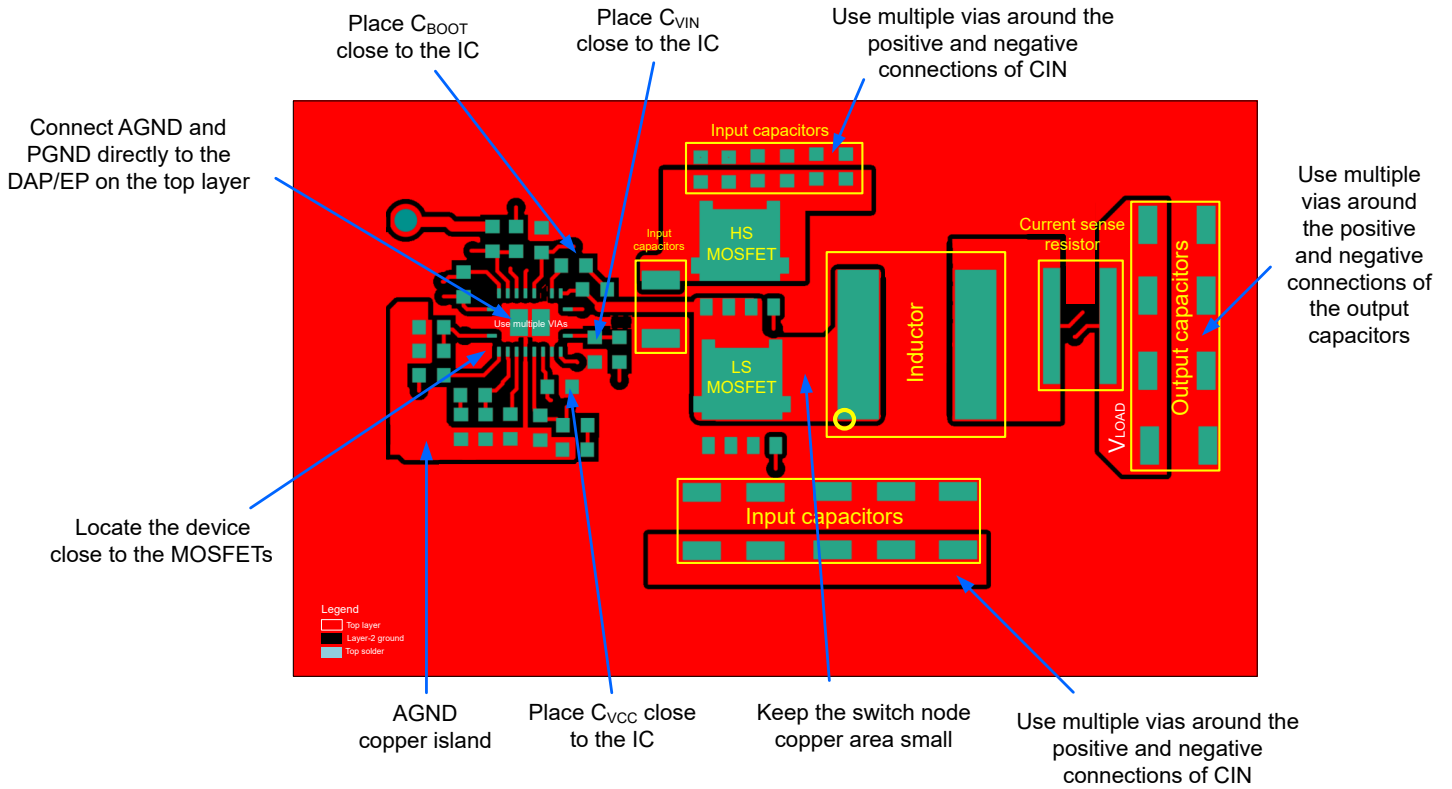


**Figure 7-16. PCB Top Layer**

## 8 Device and Documentation Support

### 8.1 Device Support

#### 8.1.1 Development Support

For development support, see the following:

- For TI's reference design library, visit [TI Designs](#)
- Technical articles:
  - [High-Density PCB Layout of DC/DC Converters](#)
  - [Synchronous Buck Controller Solutions Support Wide  \$V\_{IN}\$  Performance and Flexibility](#)
  - [How to Use Slew Rate for EMI Control](#)

### 8.2 Documentation Support

#### 8.2.1 Related Documentation

For related documentation, see the following:

- EVM user's guides:
  - Texas Instruments, [LM5190-Q1 CCCV Buck Controller Evaluation Module User's Guide](#)
- Application note:
  - Texas Instruments, [Improve High-current DC/DC Regulator Performance for Free with Optimized Power Stage Layout Application Report](#)
  - Texas Instruments, [AN-2162 Simple Success with Conducted EMI from DC-DC Converters](#)
- Analog design journal:
  - Texas Instruments, [Reduce Buck Converter EMI and Voltage Stress by Minimizing Inductive Parasitics](#)
- White papers:
  - Texas Instruments, [An Overview of Conducted EMI Specifications for Power Supplies](#)
  - Texas Instruments, [An Overview of Radiated EMI Specifications for Power Supplies](#)
  - Texas Instruments, [Valuing Wide  \$V\_{IN}\$ , Low EMI Synchronous Buck Circuits for Cost-driven, Demanding Applications](#)

##### 8.2.1.1 PCB Layout Resources

- Application notes:
  - Texas Instruments, [Improve High-current DC/DC Regulator Performance for Free with Optimized Power Stage Layout](#)
  - Texas Instruments, [AN-1149 Layout Guidelines for Switching Power Supplies](#)
  - Texas Instruments, [AN-1229 Simple Switcher PCB Layout Guidelines](#)
  - Texas Instruments, [Low Radiated EMI Layout Made SIMPLE with LM4360x and LM4600x](#)
- Seminars:
  - [Constructing Your Power Supply – Layout Considerations](#)

##### 8.2.1.2 Thermal Design Resources

- Application notes:
  - Texas Instruments, [AN-2020 Thermal Design by Insight, Not Hindsight](#)
  - Texas Instruments, [AN-1520 A Guide to Board Layout for Best Thermal Resistance for Exposed Pad Packages](#)
  - Texas Instruments, [Semiconductor and IC Package Thermal Metrics](#)
  - Texas Instruments, [Thermal Design Made Simple with LM43603 and LM43602](#)
  - Texas Instruments, [PowerPAD™ Thermally Enhanced Package](#)
  - Texas Instruments, [PowerPAD Made Easy](#)
  - Texas Instruments, [Using New Thermal Metrics](#)

### 8.3 Receiving Notification of Documentation Updates

To receive notification of documentation updates, navigate to the device product folder on [ti.com](https://www.ti.com). Click on *Notifications* to register and receive a weekly digest of any product information that has changed. For change details, review the revision history included in any revised document.

### 8.4 Support Resources

[TI E2E™ support forums](#) are an engineer's go-to source for fast, verified answers and design help — straight from the experts. Search existing answers or ask your own question to get the quick design help you need.

Linked content is provided "AS IS" by the respective contributors. They do not constitute TI specifications and do not necessarily reflect TI's views; see TI's [Terms of Use](#).

### 8.5 Trademarks

TI E2E™ is a trademark of Texas Instruments.  
All trademarks are the property of their respective owners.

### 8.6 Electrostatic Discharge Caution



This integrated circuit can be damaged by ESD. Texas Instruments recommends that all integrated circuits be handled with appropriate precautions. Failure to observe proper handling and installation procedures can cause damage.

ESD damage can range from subtle performance degradation to complete device failure. Precision integrated circuits may be more susceptible to damage because very small parametric changes could cause the device not to meet its published specifications.

### 8.7 Glossary

[TI Glossary](#) This glossary lists and explains terms, acronyms, and definitions.

## 9 Revision History

NOTE: Page numbers for previous revisions may differ from page numbers in the current version.

DATE	REVISION	NOTES
December 2024	*	Initial release

## 10 Mechanical, Packaging, and Orderable Information

The following pages show mechanical, packaging, and orderable information. This information is the most current data available for the designated devices. This data is subject to change without notice and revision of this document. For browser-based versions of this data sheet, refer to the left-hand navigation.

**PACKAGING INFORMATION**

Orderable part number	Status (1)	Material type (2)	Package   Pins	Package qty   Carrier	RoHS (3)	Lead finish/ Ball material (4)	MSL rating/ Peak reflow (5)	Op temp (°C)	Part marking (6)
<a href="#">LM25190RGYR</a>	Active	Production	VQFN (RGY)   19	3000   LARGE T&R	Yes	NIPDAU	Level-1-260C-UNLIM	-40 to 150	M25190 RGY
LM25190RGYR.A	Active	Production	VQFN (RGY)   19	3000   LARGE T&R	Yes	NIPDAU	Level-1-260C-UNLIM	-40 to 150	M25190 RGY

(1) **Status:** For more details on status, see our [product life cycle](#).

(2) **Material type:** When designated, preproduction parts are prototypes/experimental devices, and are not yet approved or released for full production. Testing and final process, including without limitation quality assurance, reliability performance testing, and/or process qualification, may not yet be complete, and this item is subject to further changes or possible discontinuation. If available for ordering, purchases will be subject to an additional waiver at checkout, and are intended for early internal evaluation purposes only. These items are sold without warranties of any kind.

(3) **RoHS values:** Yes, No, RoHS Exempt. See the [TI RoHS Statement](#) for additional information and value definition.

(4) **Lead finish/Ball material:** Parts may have multiple material finish options. Finish options are separated by a vertical ruled line. Lead finish/Ball material values may wrap to two lines if the finish value exceeds the maximum column width.

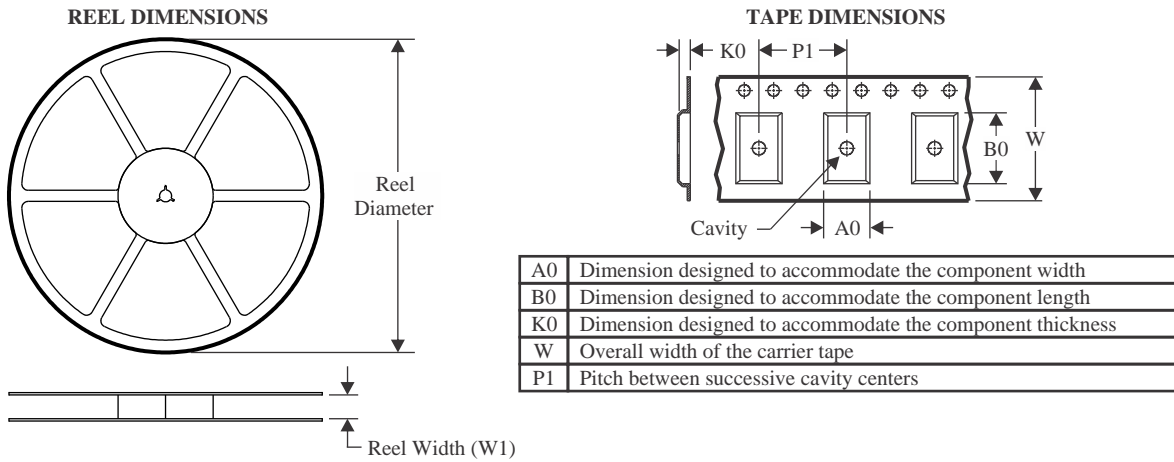
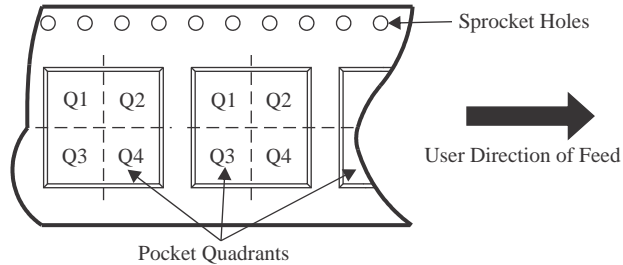
(5) **MSL rating/Peak reflow:** The moisture sensitivity level ratings and peak solder (reflow) temperatures. In the event that a part has multiple moisture sensitivity ratings, only the lowest level per JEDEC standards is shown. Refer to the shipping label for the actual reflow temperature that will be used to mount the part to the printed circuit board.

(6) **Part marking:** There may be an additional marking, which relates to the logo, the lot trace code information, or the environmental category of the part.

Multiple part markings will be inside parentheses. Only one part marking contained in parentheses and separated by a "~" will appear on a part. If a line is indented then it is a continuation of the previous line and the two combined represent the entire part marking for that device.

**Important Information and Disclaimer:** The information provided on this page represents TI's knowledge and belief as of the date that it is provided. TI bases its knowledge and belief on information provided by third parties, and makes no representation or warranty as to the accuracy of such information. Efforts are underway to better integrate information from third parties. TI has taken and continues to take reasonable steps to provide representative and accurate information but may not have conducted destructive testing or chemical analysis on incoming materials and chemicals. TI and TI suppliers consider certain information to be proprietary, and thus CAS numbers and other limited information may not be available for release.

In no event shall TI's liability arising out of such information exceed the total purchase price of the TI part(s) at issue in this document sold by TI to Customer on an annual basis.

**TAPE AND REEL INFORMATION**

**QUADRANT ASSIGNMENTS FOR PIN 1 ORIENTATION IN TAPE**


\*All dimensions are nominal

Device	Package Type	Package Drawing	Pins	SPQ	Reel Diameter (mm)	Reel Width W1 (mm)	A0 (mm)	B0 (mm)	K0 (mm)	P1 (mm)	W (mm)	Pin1 Quadrant
LM25190RGYR	VQFN	RGY	19	3000	330.0	12.4	3.71	4.71	1.1	8.0	12.0	Q1

**TAPE AND REEL BOX DIMENSIONS**


\*All dimensions are nominal

Device	Package Type	Package Drawing	Pins	SPQ	Length (mm)	Width (mm)	Height (mm)
LM25190RGYR	VQFN	RGY	19	3000	360.0	360.0	36.0

## GENERIC PACKAGE VIEW

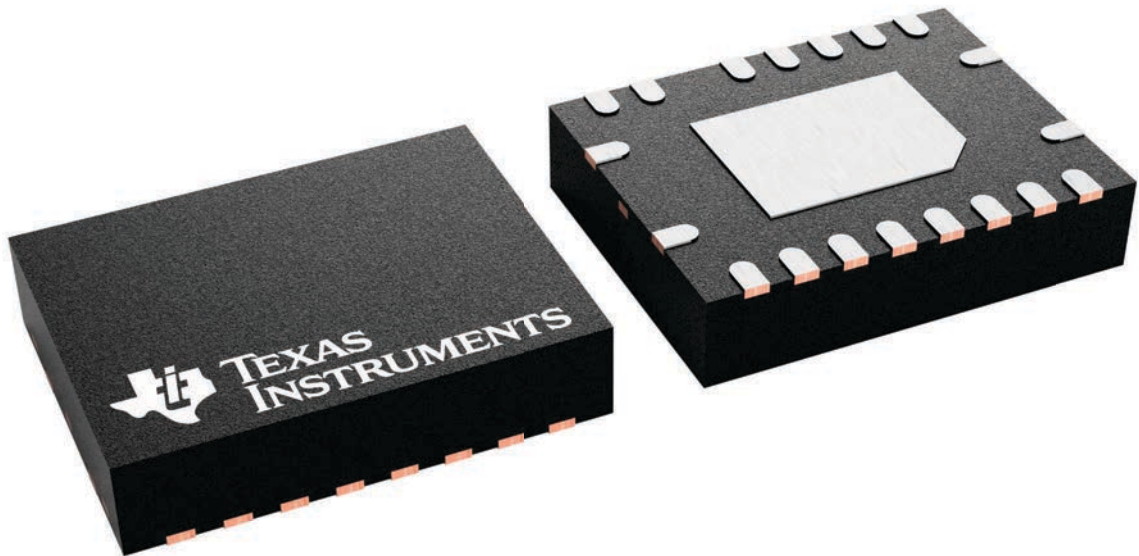
**RGY 19**

**VQFN - 1 mm max height**

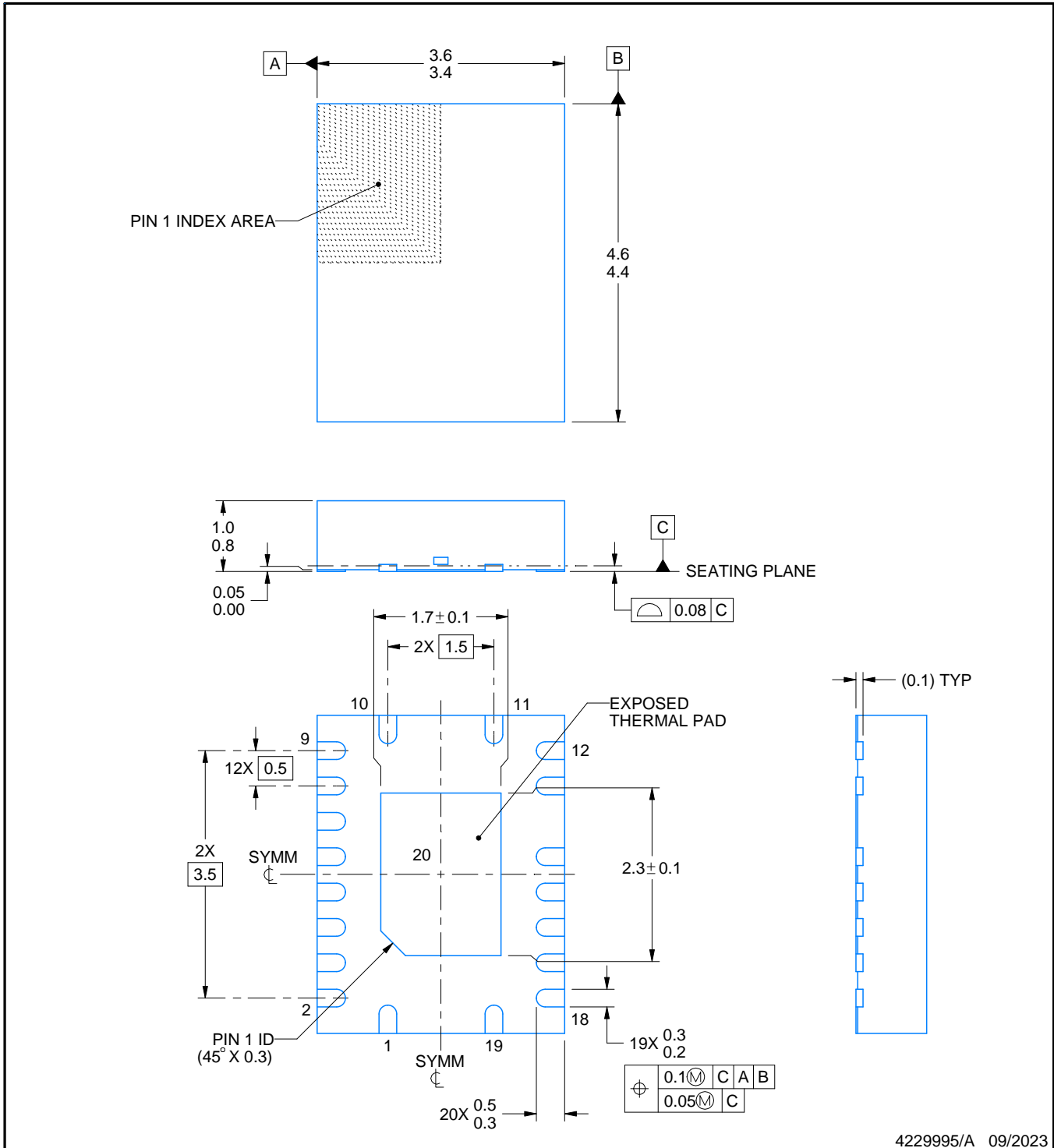
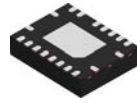
3.5 x 4.5, 0.5 mm pitch

PLASTIC QUAD FLATPACK - NO LEAD

This image is a representation of the package family, actual package may vary.  
Refer to the product data sheet for package details.



4230073/A



4229995/A 09/2023

NOTES:

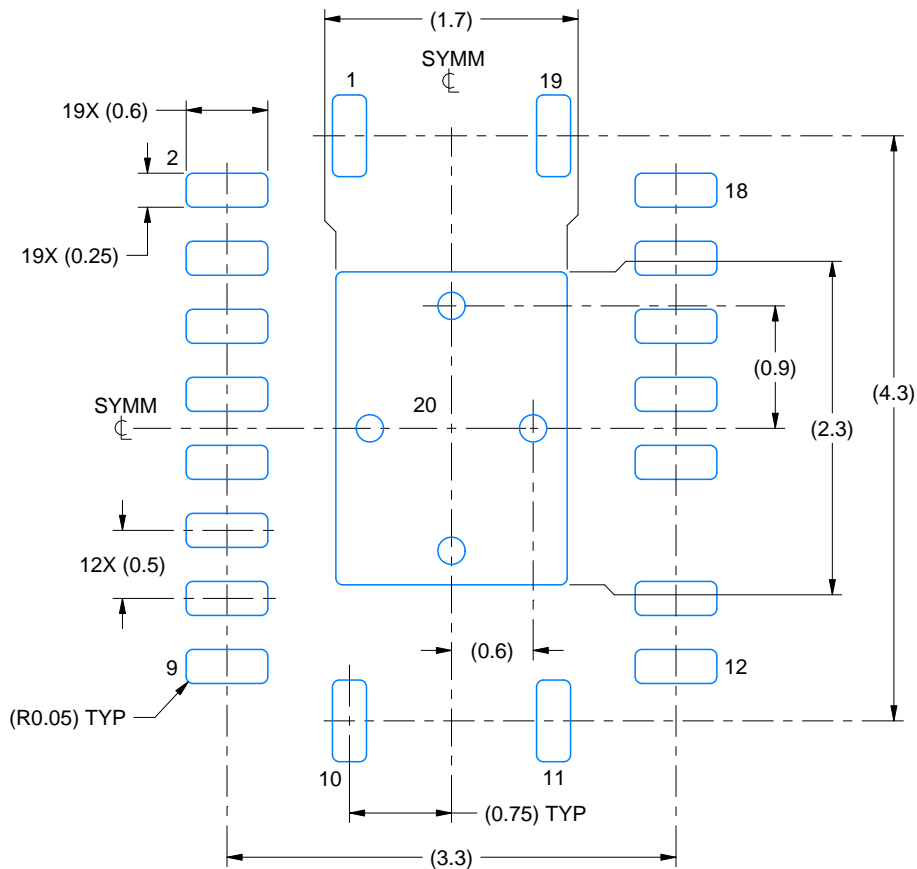
1. All linear dimensions are in millimeters. Any dimensions in parenthesis are for reference only. Dimensioning and tolerancing per ASME Y14.5M.
2. This drawing is subject to change without notice.
3. The package thermal pad must be soldered to the printed circuit board for thermal and mechanical performance.

# EXAMPLE BOARD LAYOUT

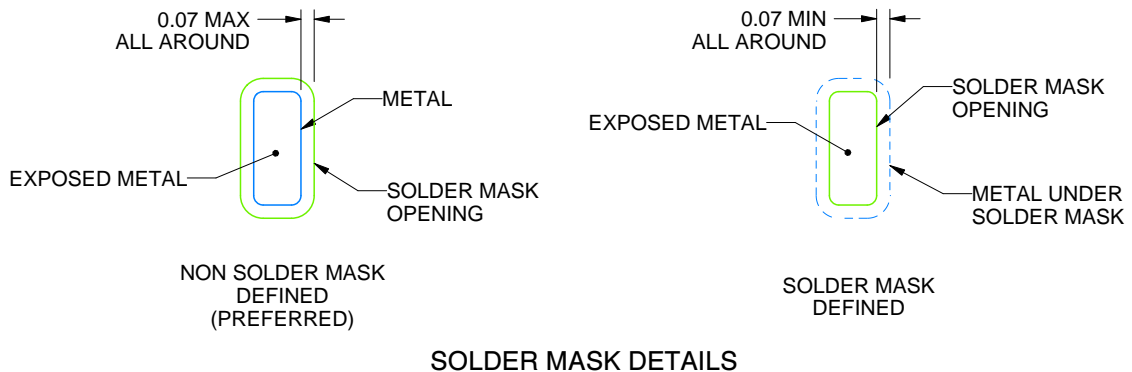
RGY0019A

VQFN - 1 mm max height

PLASTIC QUAD FLATPACK - NO LEAD



LAND PATTERN EXAMPLE  
EXPOSED METAL SHOWN  
SCALE:18X



SOLDER MASK DETAILS

4229995/A 09/2023

NOTES: (continued)

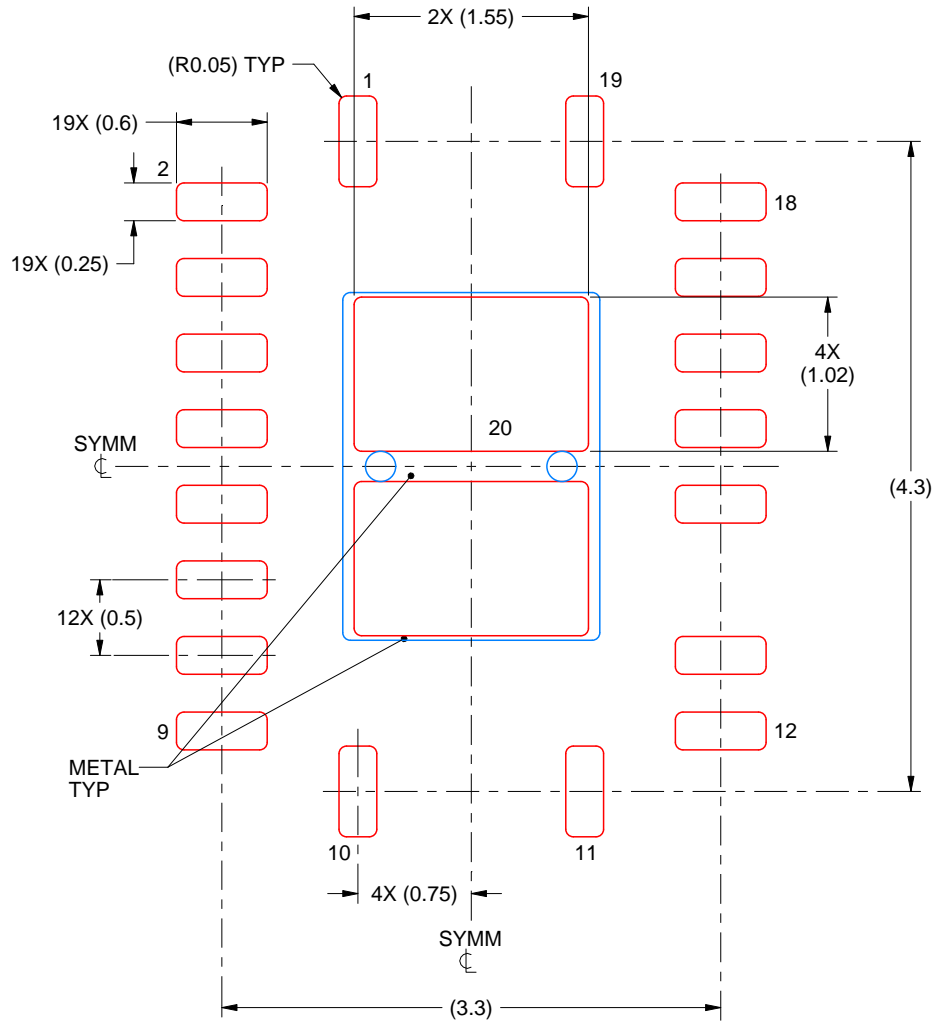
4. This package is designed to be soldered to a thermal pad on the board. For more information, see Texas Instruments literature number SLUA271 ([www.ti.com/lit/sluea271](http://www.ti.com/lit/sluea271)).
5. Vias are optional depending on application, refer to device data sheet. If any vias are implemented, refer to their locations shown on this view. It is recommended that vias under paste be filled, plugged or tented.

# EXAMPLE STENCIL DESIGN

RGY0019A

VQFN - 1 mm max height

PLASTIC QUAD FLATPACK - NO LEAD



SOLDER PASTE EXAMPLE  
 BASED ON 0.125 mm THICK STENCIL

EXPOSED PAD 21  
 81% PRINTED SOLDER COVERAGE BY AREA UNDER PACKAGE  
 SCALE:20X

4229995/A 09/2023

NOTES: (continued)

6. Laser cutting apertures with trapezoidal walls and rounded corners may offer better paste release. IPC-7525 may have alternate design recommendations.

## IMPORTANT NOTICE AND DISCLAIMER

TI PROVIDES TECHNICAL AND RELIABILITY DATA (INCLUDING DATASHEETS), DESIGN RESOURCES (INCLUDING REFERENCE DESIGNS), APPLICATION OR OTHER DESIGN ADVICE, WEB TOOLS, SAFETY INFORMATION, AND OTHER RESOURCES "AS IS" AND WITH ALL FAULTS, AND DISCLAIMS ALL WARRANTIES, EXPRESS AND IMPLIED, INCLUDING WITHOUT LIMITATION ANY IMPLIED WARRANTIES OF MERCHANTABILITY, FITNESS FOR A PARTICULAR PURPOSE OR NON-INFRINGEMENT OF THIRD PARTY INTELLECTUAL PROPERTY RIGHTS.

These resources are intended for skilled developers designing with TI products. You are solely responsible for (1) selecting the appropriate TI products for your application, (2) designing, validating and testing your application, and (3) ensuring your application meets applicable standards, and any other safety, security, regulatory or other requirements.

These resources are subject to change without notice. TI grants you permission to use these resources only for development of an application that uses the TI products described in the resource. Other reproduction and display of these resources is prohibited. No license is granted to any other TI intellectual property right or to any third party intellectual property right. TI disclaims responsibility for, and you fully indemnify TI and its representatives against any claims, damages, costs, losses, and liabilities arising out of your use of these resources.

TI's products are provided subject to [TI's Terms of Sale](#), [TI's General Quality Guidelines](#), or other applicable terms available either on [ti.com](#) or provided in conjunction with such TI products. TI's provision of these resources does not expand or otherwise alter TI's applicable warranties or warranty disclaimers for TI products. Unless TI explicitly designates a product as custom or customer-specified, TI products are standard, catalog, general purpose devices.

TI objects to and rejects any additional or different terms you may propose.

Copyright © 2025, Texas Instruments Incorporated

Last updated 10/2025

## Looking for pricing, stock, or lifecycle information?

Click below to explore more details on WIN SOURCE:

 [View MT9101A on WIN SOURCE](#)

 [NOVOSENSE](#) Information

## Optimize Your Supply Chain with WIN SOURCE Solutions

-  Global Sourcing Solution
-  Obsolete Management
-  Cost Control Management
-  Shortage Management
-  Alternative Solution
-  Excess Inventory Management